1. High sound amplitude with dark images
2. Low sound amplitude with light images
3. Variable sound amplitude with sporadic contrast

In reference with FDC observation results, each item corresponds to outcrop of the bottom rock, surface sediments and thin sediments over the rock, respectively. Among them, sporadic contrast images indicate variation of sediments thickness and angulation of the sea bottom, varying from dark to light in many changes.

In MBES acoustic reflection image, there are dark colored belt shape anomaly running in NNE–SSW direction in the central part of the survey area. The maximum width of the anomalous belt is about 10 km. This outcrop of the basement rock is assumed to be due to a spreading center judging from the existing data. This outcropped rock runs from the center of the northern end of the survey area towards south, locally overlapping or partly curving a little towards the southern end of the survey area.

In the whole survey area, light image part, indicating thin sediments over the rock is predominant. Also, narrow belt shaped outcrops in parallel with spreading center are seen in several places.

Especially, in close view of outcrops (dark part), the following points are raised in relation to submarine topography;

Outcrop of the central spreading center corresponding with generally furrow zone from the northern end to the vicinity of 20 ° 38'S. Contrary, from 20 ° 38'S to the southern end of the survey area, it corresponds to the topographic high.

In the eastern side of the spreading center from the central survey area to the southern part, belt shaped outcrops in several places correspond to seamounts or knoll chains and their steep slope parts.

In the southern part of the survey area, in the vicinity of 21 ° 2'S, 176 ° 38'W, 21 ° 24'S, 176 ° 49'W and the western side of the spreading center wide areas of outcrop are seen and correspond to various seamounts and knoll chains.

In comparison with the southern part of the survey area, seamounts and knoll chains in the northern part of the area do not show much dark images, which suggests that this area is widely covered with sediments.

Also, compared the western side with the eastern side, where sediments are predominant, more detail dark and light contrast are recognized in the west side. This is considered to reflect complicated topographical angulation in detail.

(3) nSBP Survey

The main objectives of nSBP survey were to study distribution of comparatively shallow deposits

(about several ten meters) and to understand topographical and geological features of the sea bottom such as faults and folding from the reflection records. This method is most powerful when the topography is generally flat and the layered structures are expected in the sea area.
Frequency of the signal is 3.5 kHz, which is rather lower than the other sounders, so that the penetration depth below the sea bottom is deeper than the others, while the transmitting beam angle is large because of low frequency signal and technical restrictions of the instrument. So, it has been pointed out that the reflected signals from the bottom are not only from the bottom below the vessel.

The nSBP system should be adopted in the flat field like as ferromanganese sea area, however, nSBP survey was carried out to examine adoptability of this system, which has a narrow transmitting beam angle, in the sea area like this.

Survey with various ocean floor topographies such as volcanoes, seamounts, and hydrothermal ore deposit, and continuous data were collected along the all survey lines for data processing and analysis.

1) Data acquisition and processing

Data acquisition was made simultaneously with bathymetric survey by using single mode, 4 pulse signals at a speed of 10 knots. Good quality data with high S/N ratio were collected over the entire sea area without any resetting of the system parameters such as signal strength and pulse. However, due to the limitation of the beam angle, no records were collected in the slope area of more than four degrees, so that little data was recorded over the western side of the sea area where mountainous topography is dominant.

During data processing, several typical patterns of nSBP record were defined, then every one minute record on the chart was classified to plot its pattern on the survey lines and a plan map was made showing the type of the record. Bathymetric map was overprinted on the plan map to know the relation of the type with topography.

To make a plan map, considering line interval and speed of vessel, one data set (for every one minute) represents the area of 130 m in east and west, and 1200 m in north and south, and each rectangular area was color coded depending on their type.

Definitions of the type were decided based on the following points:

(1) Whether reflection data from the ocean bottom are observed
(2) Whether the layered structures are seen and how is the reflecting intensity (transparency or semitransparency)
(3) Topographic change

Records of nSBP are mostly different from the conventional SBP records, so that the classifications were made independently from the SBP. The results of each type are shown in Fig. 3-4-4.

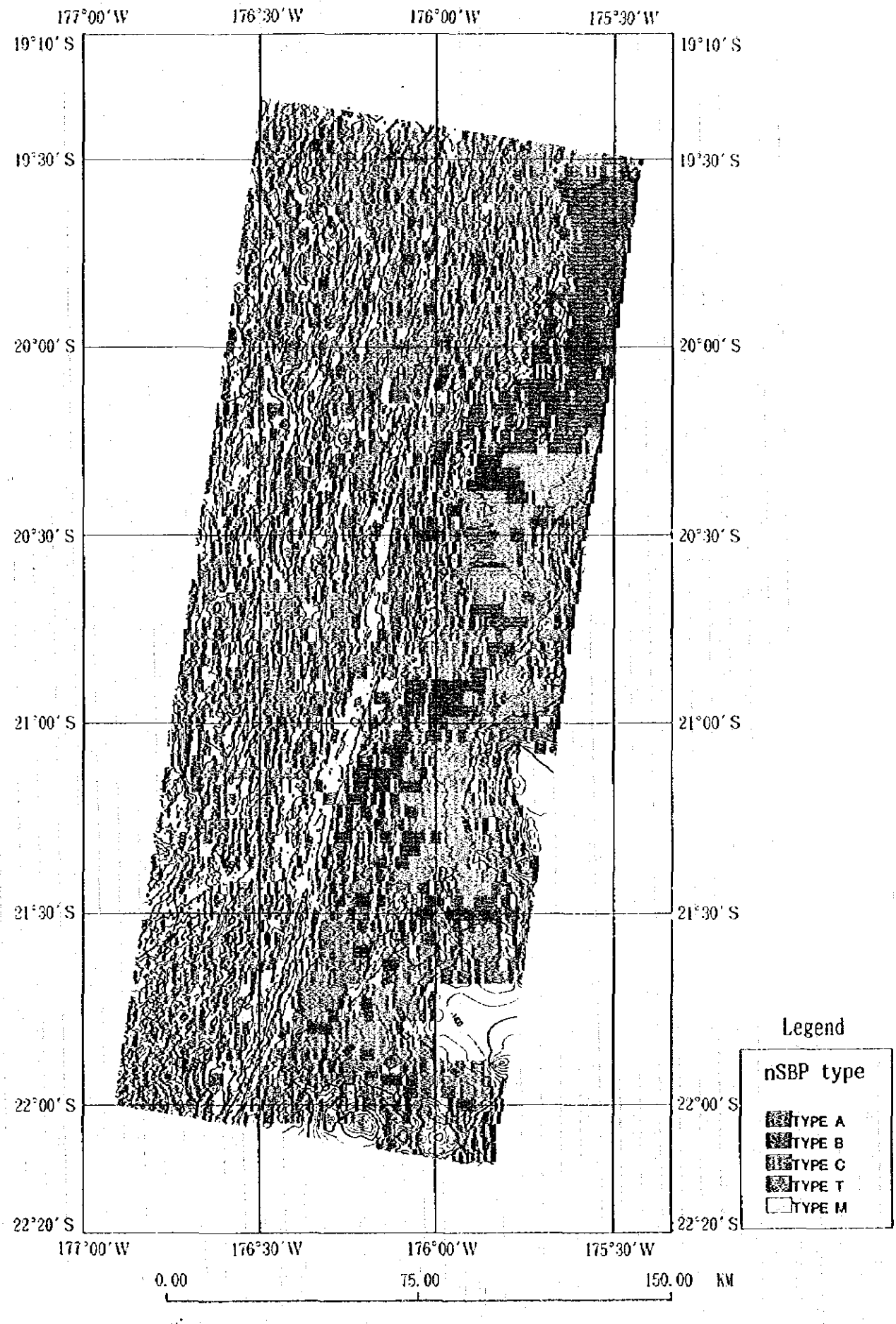

Fig. 3-4-4 Distribution map of nSBP type

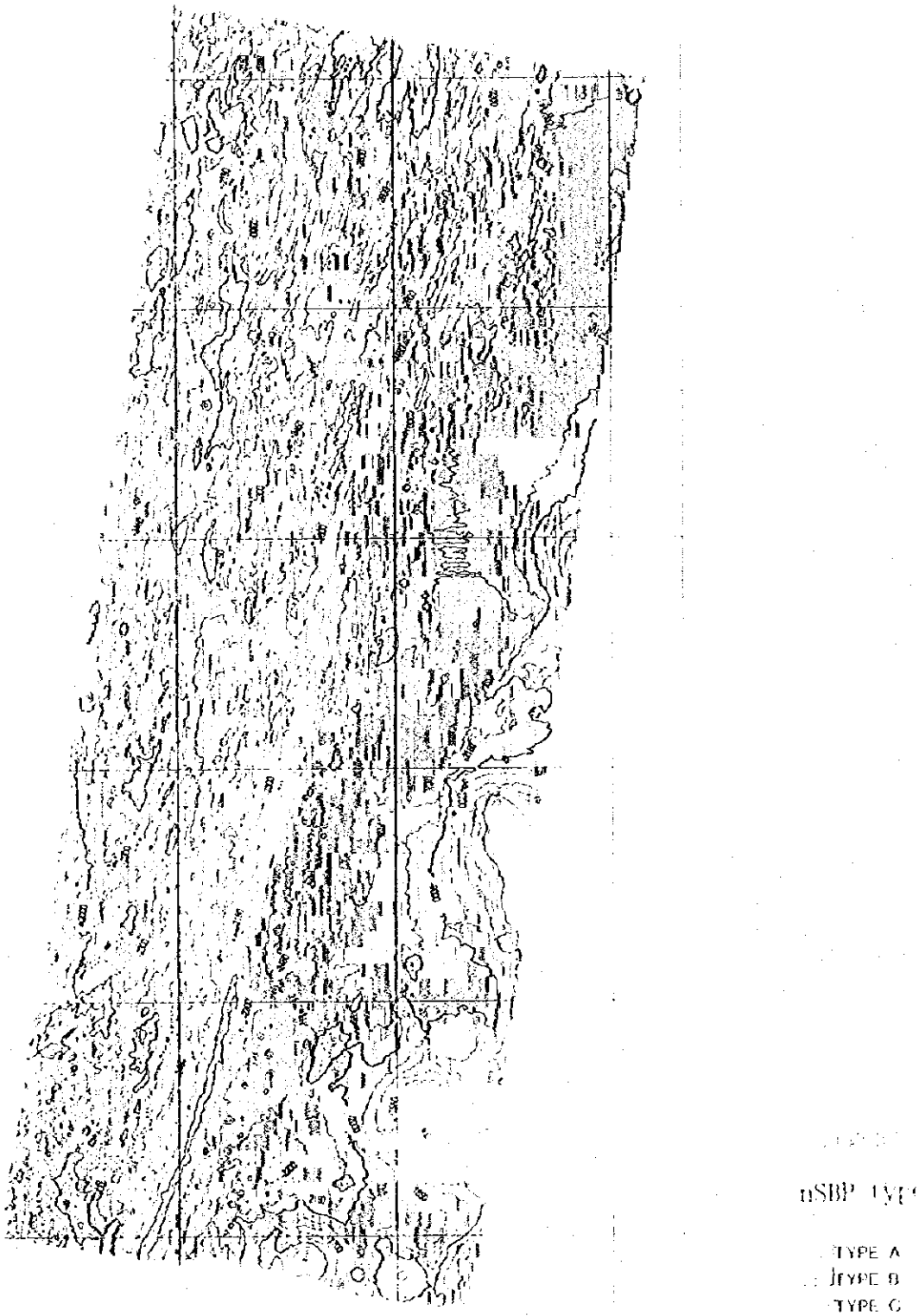

Fig. 3.1.1 Distribution map of nSBP type

Especially in the West of the sea area, definition from the record was so hard that the following four groups are adopted. Typical records for each type are shown in Fig. 3-4-5.

Type A: Sea bottom is clearly detected under which multiple layered (3 to 6 layered) structures are also read. Characteristic patterns of this type are mostly semi transparency data in between the layers and partly no reflection data showing transparency layer. Recording width (penetration depth) is more than 20 m.

Type B: Sea bottom is clearly detected under which 2 – 3 layered structure are seen. Basic pattern is the same as Type A, but the recording width is less than 20 m. Thickness of layers for both types A and B is easily identified as around 5 – 10 m.

Type C: Sea bottom can be clearly identified, but no clear difference between transparent and semi transparent layer under the bottom. For this type, distinction of layer is generally difficult and some are clearly transparent but the others are a mixture of semi transparent layer. This vague pattern is typical in a slope area due to decrease of reflecting signals from the slope.

Type T: Only sea bottom is clearly identified and the thickness of the layer is rather thick (about 5 m). This type indicates strong reflecting record, showing transparent on the chart record in the lower part. This pattern is often seen in an area with gentle slopes.

Type M: No clear record of reflection or no record at all is observed due to steep topography.

2) Consideration on distribution of nSBP type

As a whole, distributions of nSBP type are clearly separated into two groups in the eastern and the western side of the spreading center which runs in north-south direction in the center of the sea area. In the eastern side, types A, B and T are dominant and in the western side, types C and M are widely seen. These types suggest that generally flat areas are seen in the eastern side and comparatively rugged terrain in the western side of the spreading center, basically reflecting the general topographic features, but not so much as SBP capability as far as the plan map is concerned. However, in the eastern part of the sea area where flat topography is seen, very detail layered structure can be analyzed from the record along the survey lines, which is very useful data to know distribution of sediments. In more detail, Types A and B are partly seen in the western mountain area, which suggest the distribution of sediments. This means that even in the mountain area, small scale sporadic distribution of sediments could be detected by small beam angle. Therefore, it is clear that horizontal resolution is good enough.

Concerning to MBES acoustic reflection image, nSBP patterns are concordant with MBES acoustic reflection image. The MBES acoustic reflection image apparently shows different dark and light distribution in east and west of the spreading center, showing in most part of the eastern side flat

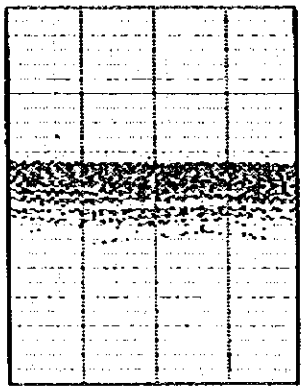

TYPE : A

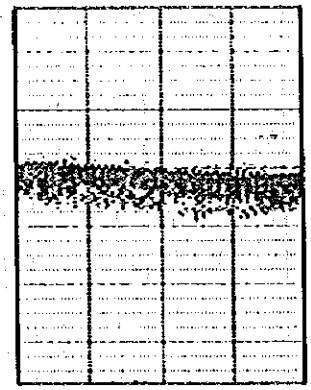

TYPE : B

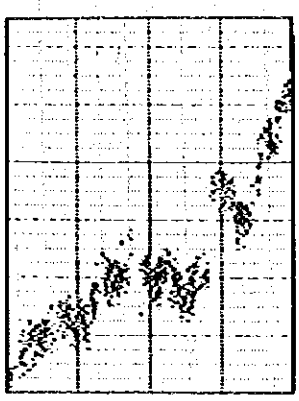

TYPE : C

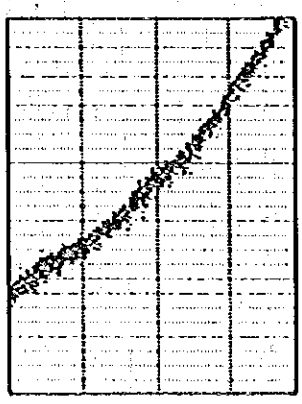

TYPE : T

Fig. 3-4-5 Typical records for each type

contrast with little change and in the western side complex change in contrast although with a little change in sound pressure. These changes are considered to be reflecting complex change in the bottom surface and their texture. The nSBP map coincides well with the MBES acoustic reflection image; the eastern side is flat showing types A and B which suggest the distribution of sediments and the western side shows type C which suggests the complicated topography.

In addition to this, in the northeastern part of the sea area where pattern A is seen, about 2.5 m length core sample was collected by LC, and it is observed that brown clay is interbedded by over ten layered volcanic sandy sediments. The nSBP record taken on this site shows 6 to 7 layered structure and the thickness to the lowest part is estimated about 30 m. The first layer shows semi transparent layer. If sediments consist of homogeneous grains, no reflection occurred in the layer and it will be reflected as the transparent layer. However, judging from this core sample, it is assumed that many sand stones played complicated reflectors showing semi transparent layer on the record. Also in the eastern sea area where types A and B are widely distributed, most records from the upper layer show semi transparent layer, suggesting the same circumstances as mentioned above.

Submarine hydrothermal ore deposits are often found in the so called volcanic zone where submarine hydrothermal venting and spreading center are seen. From the view point of exploration, the nSBP survey could not be a direct exploration method, because no good quality data or poor quality data are obtained over the sloped area. However, capability of delineating distribution of sediments and its layer structure is very effective in decision of sampling points and understanding regional volcanic activities, which could be used as a supplementary tool for hydrothermal ore deposit exploration.

CHAPTER 4 ORE DEPOSITS INVESTIGATION

4-1 General

Several hydrothermal ore deposits and active chimneys were discovered in the southernmost part of the survey area and the adjoining southern extension of the area (Y.Fouquet et al., 1993). All of these mineralizations are observed on the top of the ridge as the spreading center.

High sound amplitude zone in the MBES acoustic reflection image corresponds to the outcrop of the rock, which is considered to be the most promising area for the new volcanic activity. In the survey area, these zones are the spreading center consisting of grabens and ridges running through the center of the area, fault cliffs in the vicinity of the spreading center, knolls in the eastern part of the area, and horsts and knolls in the western part of the area.

Ore deposits exploration in this survey was especially focused to the spreading center and the zone where new volcanic rocks distribute, since the above mentioned known deposits were found near the spreading center and are still active even now. Furthermore, characteristic geological features were selected as a target. Taking a regional difference into consideration, we tried to conduct the survey over the entire area as possible.

The ore deposits investigation consists of FDC survey, SSS survey and sampling by LC, FPG and CB. Firstly, the FDC survey was carried out in order to observe sea floors, to study the features of volcanic rocks, muddy sediments and geological structures, furthermore to find mineralization and ore deposits. Also, the SSS survey was conducted as a supplementary method to study the precise sea floor topography. On the basis of the results of the FDC observation and MBES acoustic reflection image, sampling survey was carried out. The area of the ore deposits investigation and the location maps of surveys are shown in Fig. 4-1-1 and 4-1-2 (1)-(4) respectively.

By the FDC survey, sea floor observation was selectively made for the spreading center and the overlapping spreading center which form a graben in the center of the area, and the spreading center which forms a ridge in the central to southern part of the area. Sea floor observation was also made for seamount chains in the east of the spreading center and mountain area in the southwestern part of the area.

The SSS survey confirmed the precise topography and the geological structure of the spreading center and the overlapping spreading center which form a graben in the center of the area. The FDC survey followed by the SSS survey verified the concordance of the SSS images with real sea floor topography and submarine geology.

The objective of LC sampling is basically to collect muddy sediments as basic data for the geochemical survey. Sampling was made near the spreading center which forms a graben and its eastern side in the north of the area, and in the spreading center which form a graben in the central north. In the

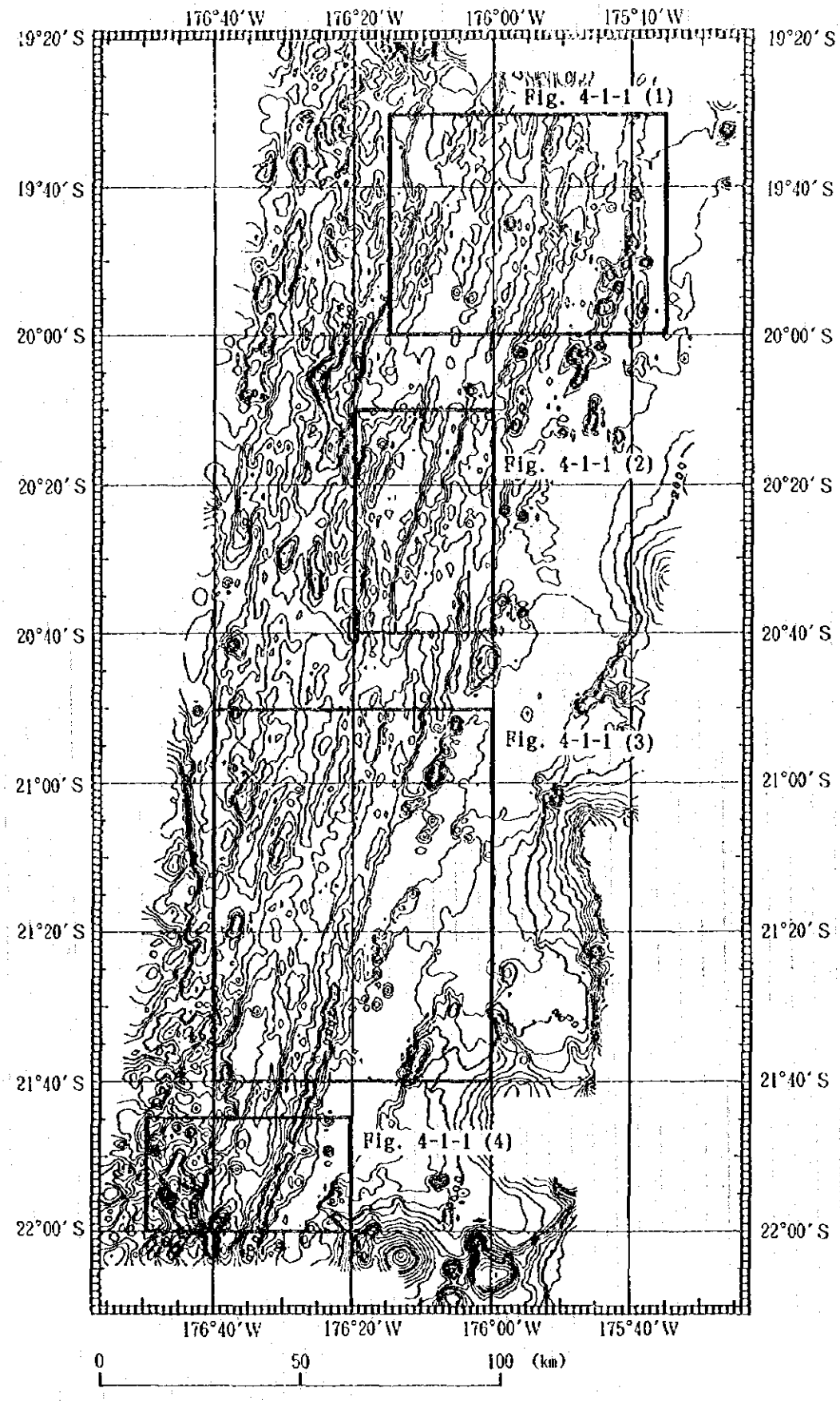

Fig. 4-1-1 Area map of location maps of ore deposits investigation

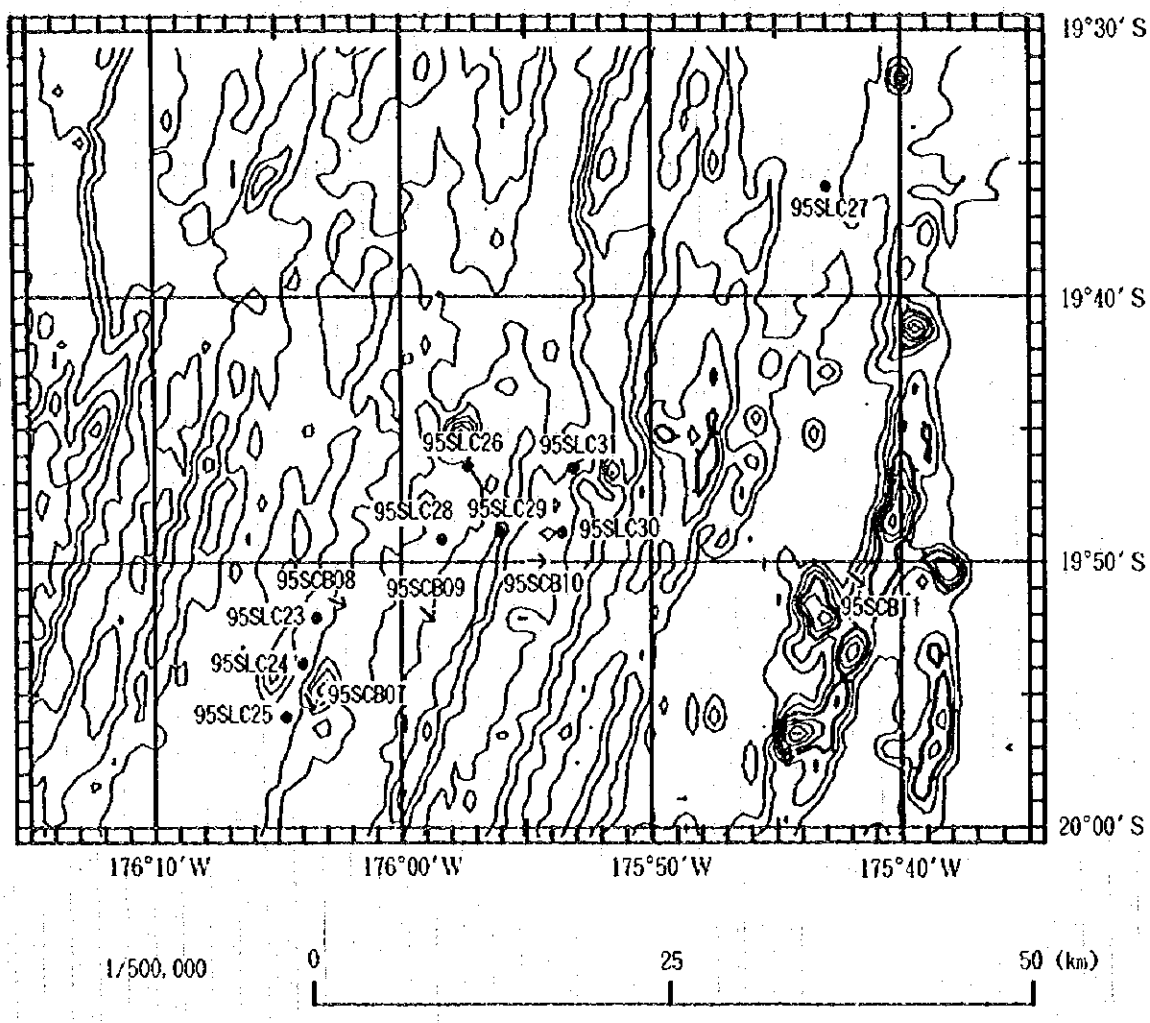

Fig. 4-1-2 (1) Location map of ore deposits investigation

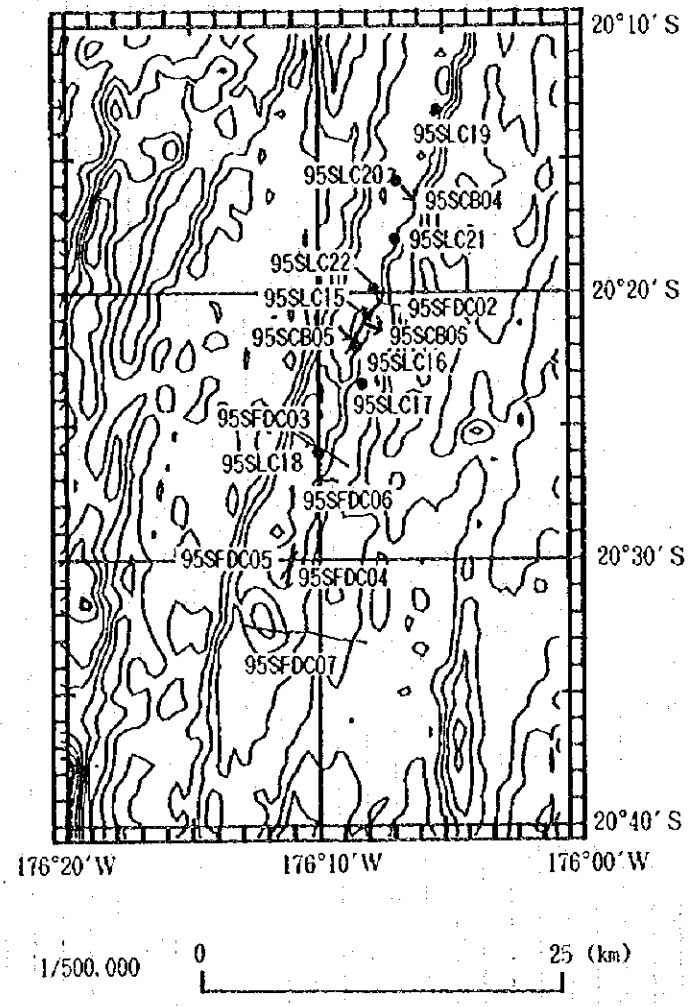

Fig. 4-1-2 (2) Location map of ore deposits investigation

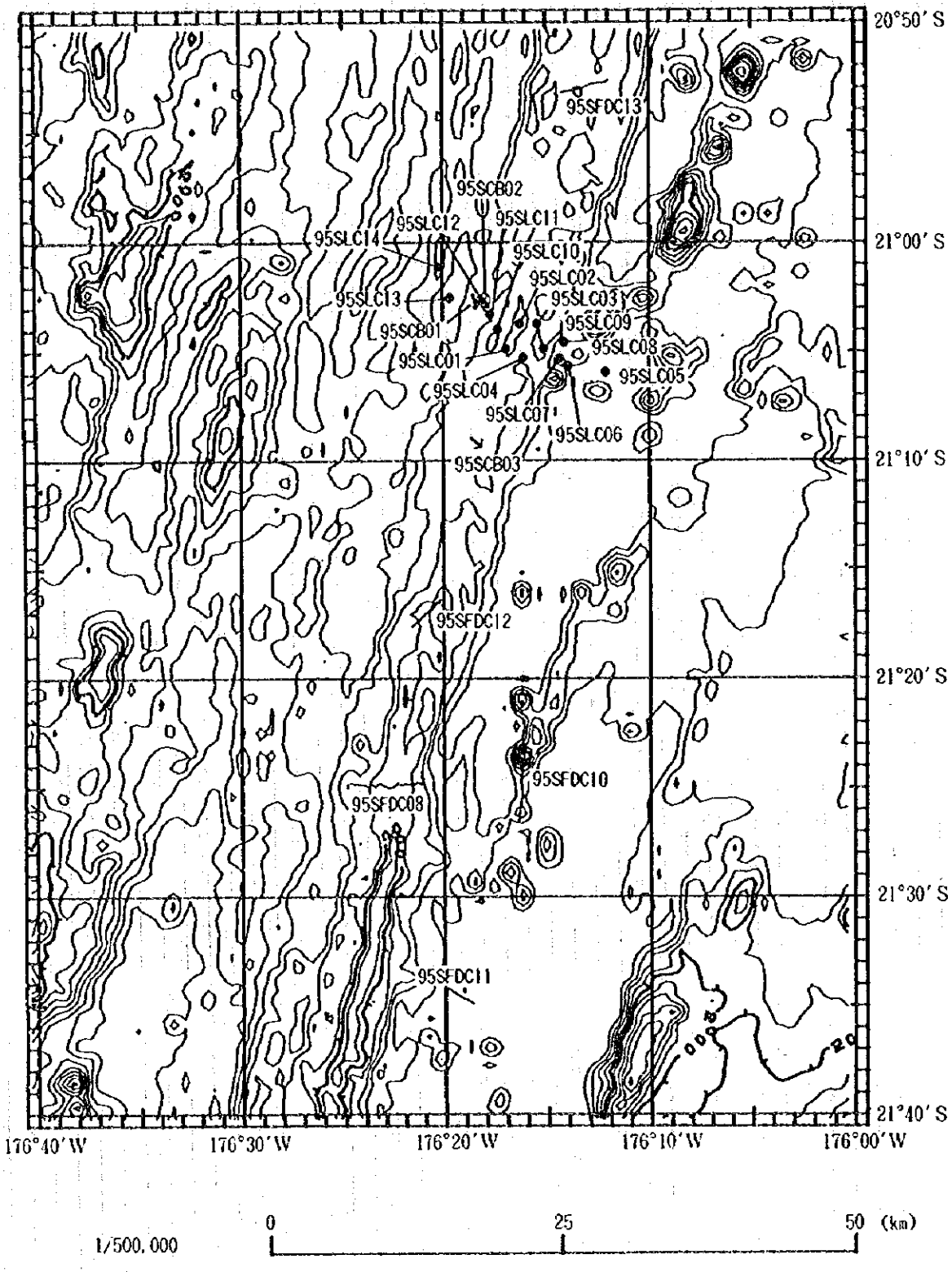

Fig. 4-1-2 (3) Location map of ore deposits investigation

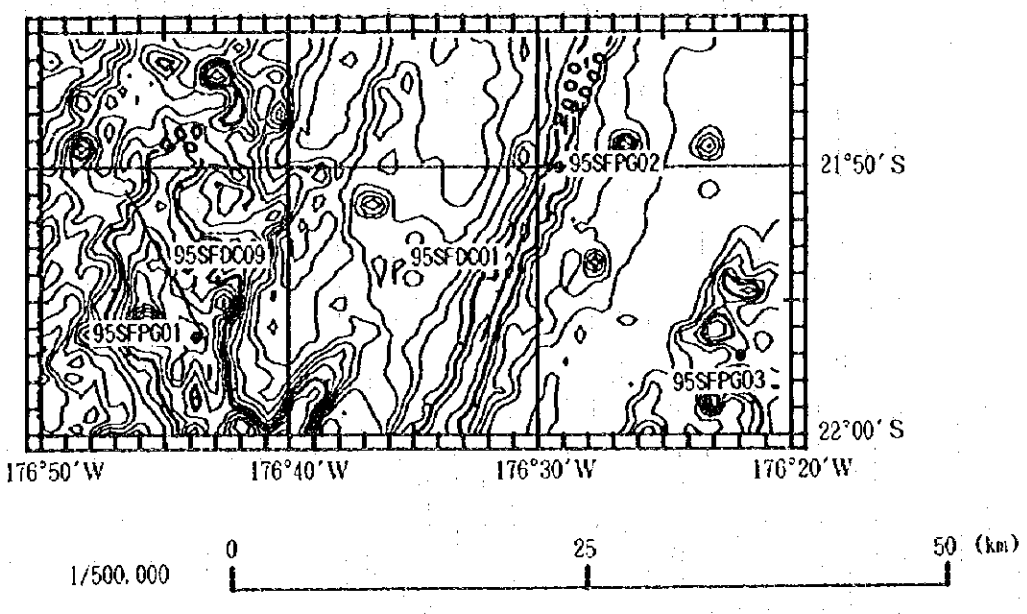

Fig. 4-1-2 (4) Location map of ore deposits investigation

central south, sampling was made on horsts and grabens crossing over the spreading center.

The objective of the FPG sampling is to collect lava samples at the characteristic points in the southernmost part of the survey area. Sampling was made on the steep ridge of the spreading center, the mountain area in the west of the spreading center and the knoll chain in the east of the spreading center.

The objective of the CB sampling is to collect lava in the spreading center. Sampling was made on the outcrop detected by the MBES acoustic sounding bathymetry, mainly in the northern part of the area.

4-2 SSS Survey

The SSS survey, with a purpose of studying submarine precise topography and distribution of sediments, was carried out at three track lines over the overlapping spreading center in the central part of the survey area, where outcrops and fractured zones exist and possible hydrothermal activities are expected. In setting the track lines, results of strong reflected signals by the MBES acoustic reflection images which were assumed to be due to the outcrop were considered. The SSS track lines and image maps are shown in Fig. 4-2-1 (1)-(3).

According to the results, several characteristic records indicating submarine precise topography were obtained. Large or small scale faults structures, very strong reflecting signals which indicate wide spreading outcrops, mound shaped structure or plume as a sign of hydrothermal activity and so on were observed. The detailed topographic structure was clarified by this method, helping estimate the potential hydrothermal activities in the survey area.

The results of each track line are as follows;

(1) Line 95SSS01

Fault-like records were observed in the vicinity of 20° 17'S, 20° 22'S and 20° 29'S. Near 20° 20'S, sounding record was detected showing an outcrop with a diameter of about 25 m within a furrow-like structure with a diameter of about 110 m. On the whole area, strong reflecting sound signals were recorded from the slope of the propagating spreading center, which are deemed to be due to outcrop of the rock. However, by the FDC, abundant marine sediments were observed, but no eminent outcrop of the rock was confirmed.

(2) Line 95SSS02

This track line cuts across the overlapping spreading center in almost east-west direction. Fractured or fault-like structures are dominant on this line. Sounding records suggesting plumes were detected in the vicinity of 20° 26'S - 20° 28'S, 20° 31'S, 20° 33'S and 20° 35'S. Near 20° 26'S, a

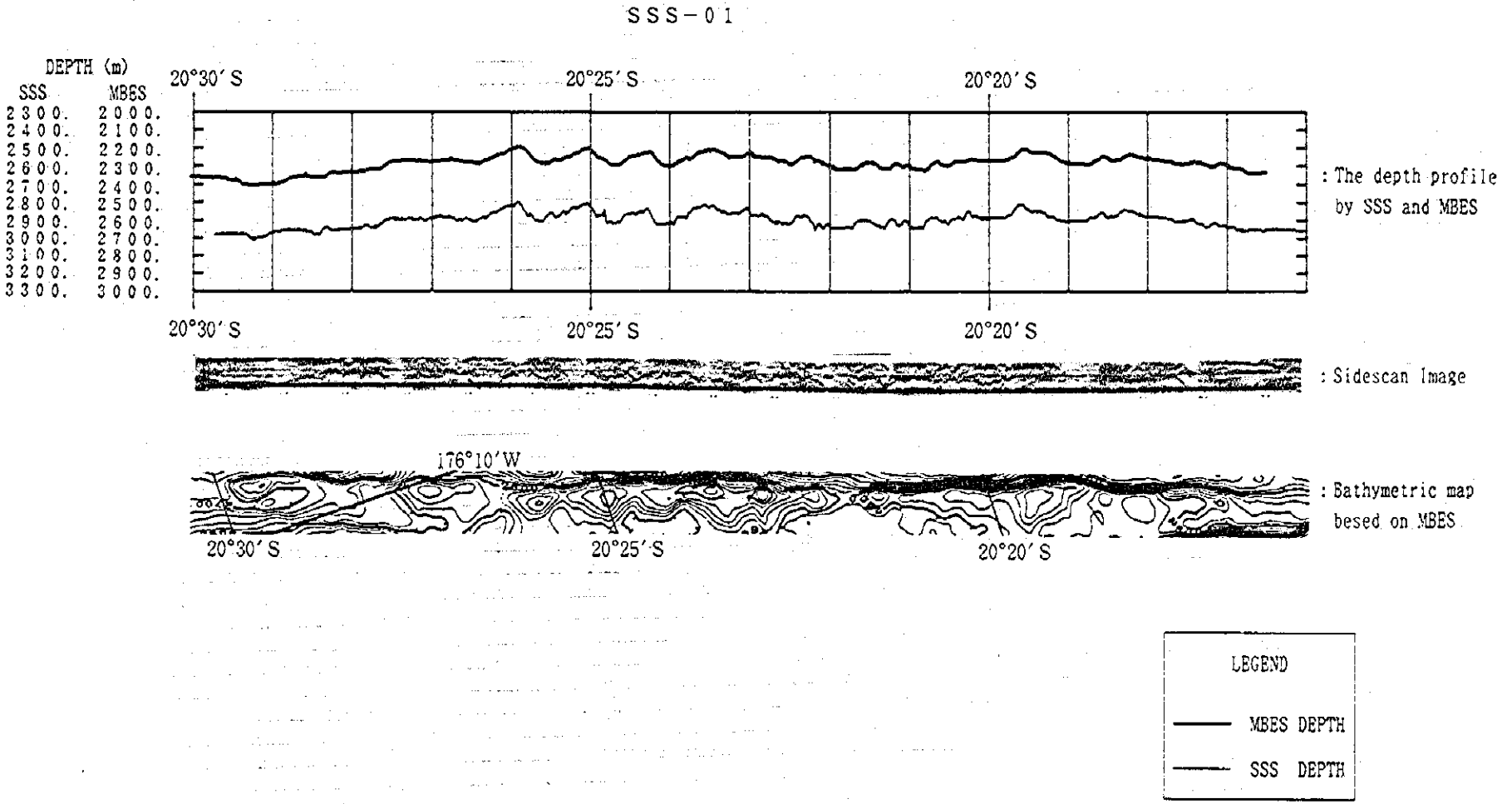

Fig. 4-2-1 (1) Results of Side Scan Sonar Survey

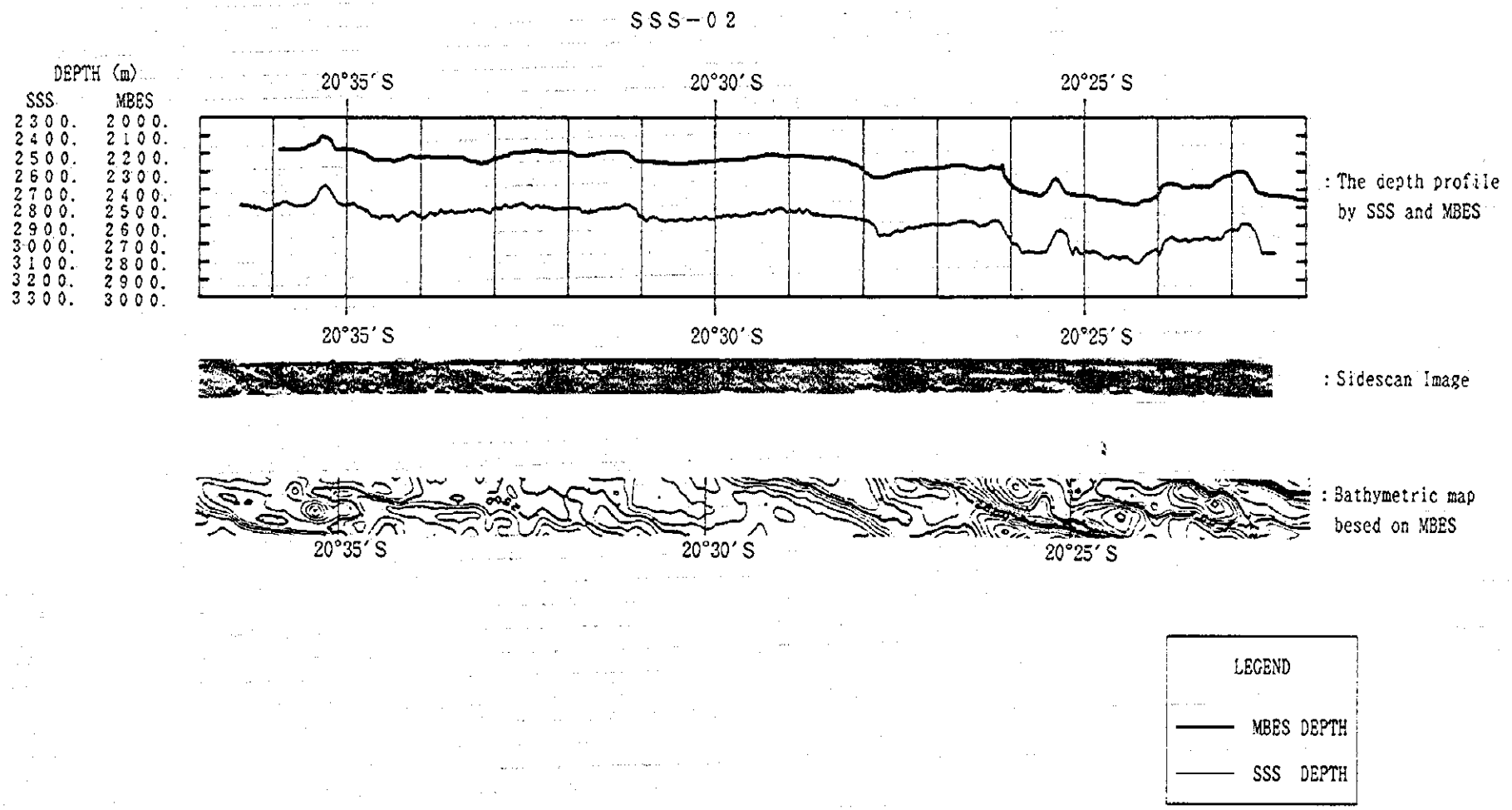

Fig. 4-2-1 (2) Results of Side Scan Sonar Survey

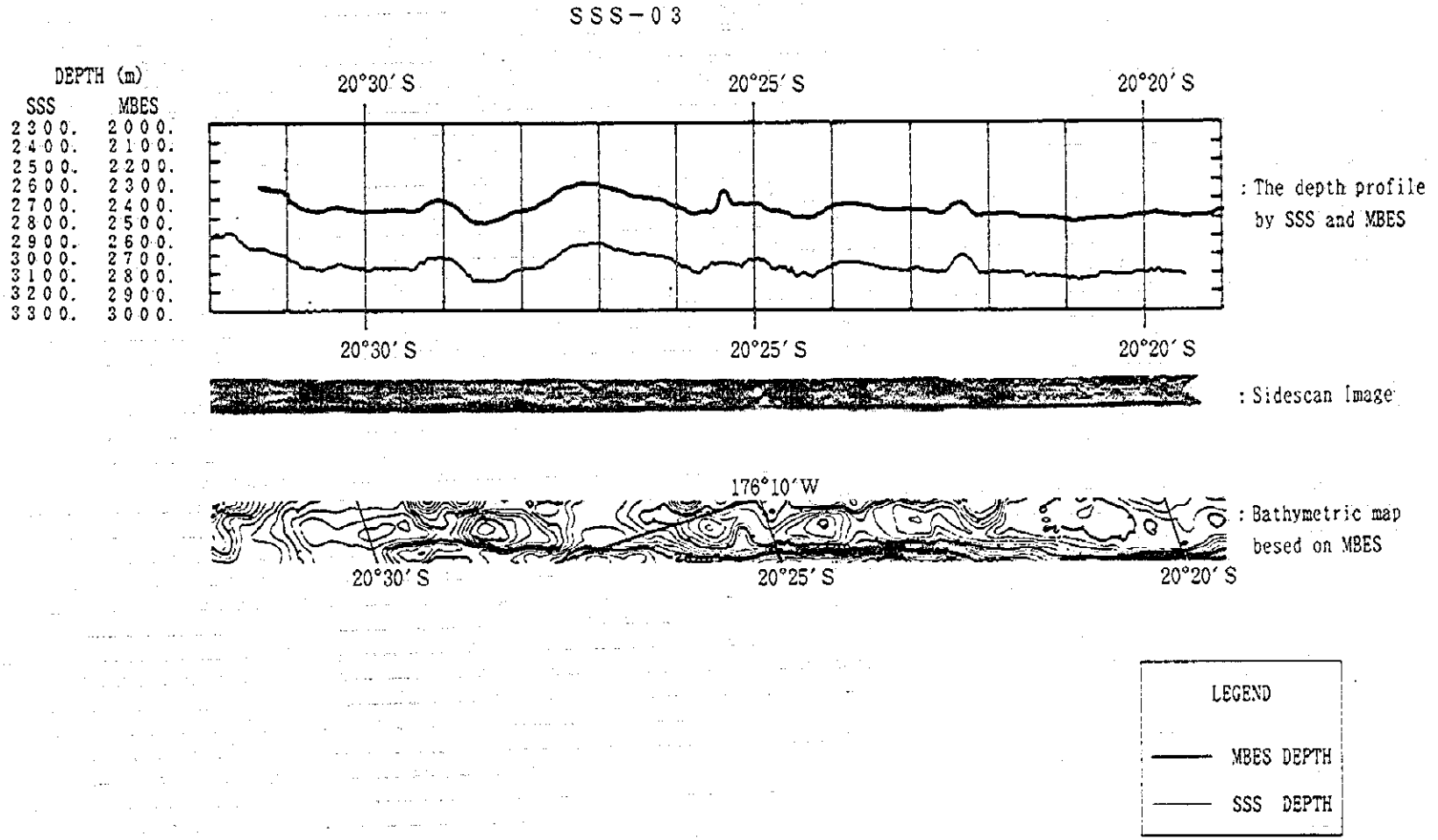

Fig. 4-2-1 (3) Results of Side Scan Sonar Survey

furrow like structure (ϕ 50–80 m) was obtained. By the FDC observation, developed fracture zone was found, but no signs of hydrothermal activity were detected.

(3) Line 95SSS03

Fractured or fault–like structures were observed in wide range of the area. Plume–like structures were also observed near 20° 20'S, 20° 21'S, 20° 22'S and 20° 30'S, however, by the FDC observation, marine sediments cover thinly the rock with no signs of hydrothermal activity.

4–3 FDC Survey

The objectives of the FDC survey are to observe submarine geology and structure, and to discover hydrothermal ore deposits. On the basis of the results of bathymetry, the MBES acoustic reflection image and SSS image map, the FDC survey was done with high priority over the spreading center in the Lau Basin, where hydrothermal ore deposits are expected to exist. Besides this, the FDC observation was also carried for characteristic seamounts and knolls. Real–time see floor observation was made through color images by towing the FDC, on which a still camera and a TV camera were also loaded.

The track lines for the FDC observation are total 13 lines; 6 lines in Block TS–C, 4 lines in Block TS–D and 3 lines in Block TS–E. As the results of observation, no hydrothermal ore deposit was discovered. As a sign of mineralization, we confirmed yellow precipitations at seven places, brown precipitations at one place, black precipitations at 10 places and white precipitations at 3 points. Each of them is local, showing no positive ore sign or indications. Two Calyptogena magnifica and two Munidopsis sp., which are often seen in an area of hydrothermal activity, were found, but are also no positive signs of hydrothermal activities. Water temperature anomalies were found at 17 points.

Locations of all FDC track lines are shown in Fig. 4–1–2 (2)–(4), and representative photos are shown in Fig. 4–3–1 (1)–(4). Route maps and the results of FDC survey are shown in Appendix Fig. 5 (1)–(13) and Appendix Table 1, respectively. The results of each track line are as follows:

1) 95SFDC01 (See Fig. 4–1–2 (4))

This line was set with the aim to confirm the known ore deposit in the south of Block TS–E and to observe the geological features in the spreading center where recent volcanic rocks are seen. The line locates along the summit of the spreading ridge. Towing direction is NNE to SSW in parallel with the spreading center, and the observation line length is 6.2 nautical miles.

On the northern part of the line, slag lava or aa lava are dominant, while in the south, pillow lava is prominent. Pillow breccia is dominant on the flat ridge in the south. Here, open cracks in width 1 to 3

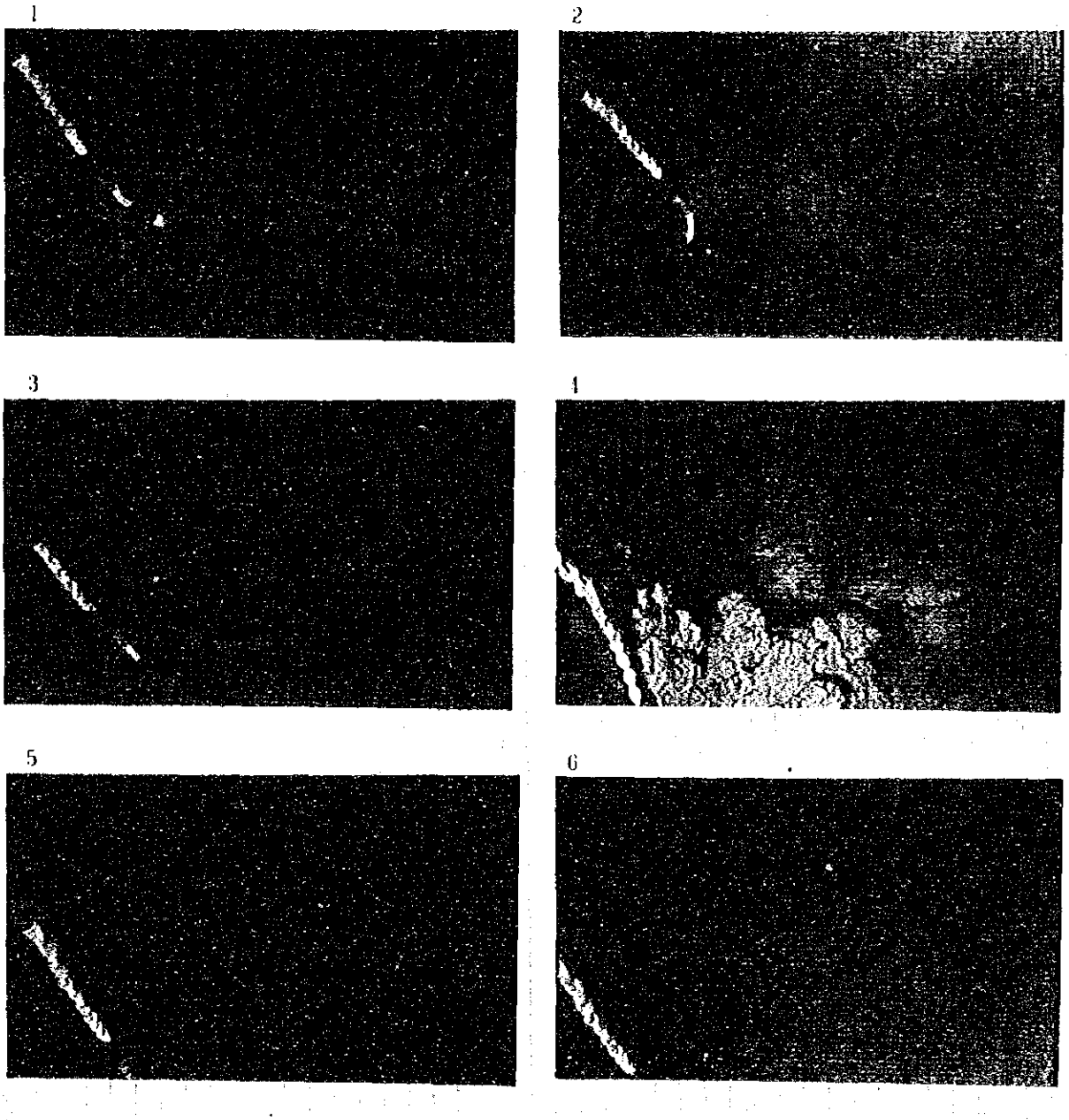

1. Pillow lava (95SFDC13 20°53.10′S, 176°13.49′W, 2,169m)
2. Pillow lava (95SFDC08 21°24.83′S, 176°23.33′W, 2,085m)
3. Brecciated lava (95SFDC02 20°22.12′S, 176°08.77′W, 2,770m)
4. Aa lava (95SFDC01 21°50.60′S, 176°29.76′W, 1,987m)
5. Pahoehoe lava (95SFDC13 20°52.95′S, 176°12.99′W, 2,227m)
6. Pahoehoe lava (95SFDC13 20°52.95′S, 176°12.99′W, 2,227m)

Fig. 4-3-1 (1) Photographs of FDC observation

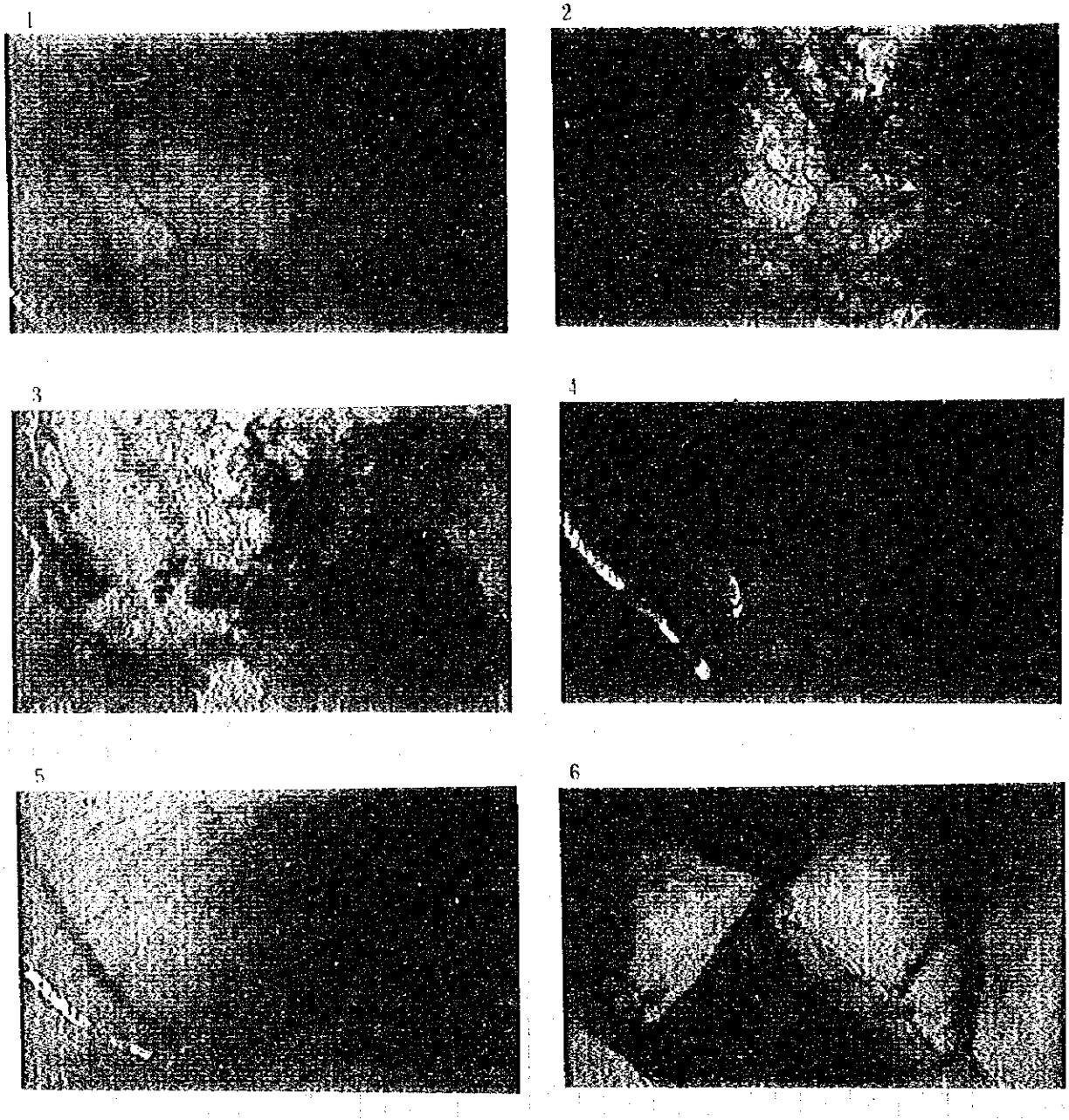

1. Sheeted lava (95SFDC12 21°17.13′S, 176°20.83′W, 2,076m)
2. Talus deposits (95SFDC01 21°51.65′S, 176°30.30′W, 1,842m)
3. Sediments of black glass (95SFDC09 21°52.76′S, 176°45.52′W, 1,736m)
4. Collapse pit (95SFDC13 20°52.93′S, 176°12.95′W, 2,224m)
5. Open fissure (95SFDC02 20°21.12′S, 176°08.20′W, 2,792m)
6. Open fissure (95SFDC02 20°22.28′S, 176°08.91′W, 2,653m)

Fig. 4-3-1 (2) Photographs of FDC observation

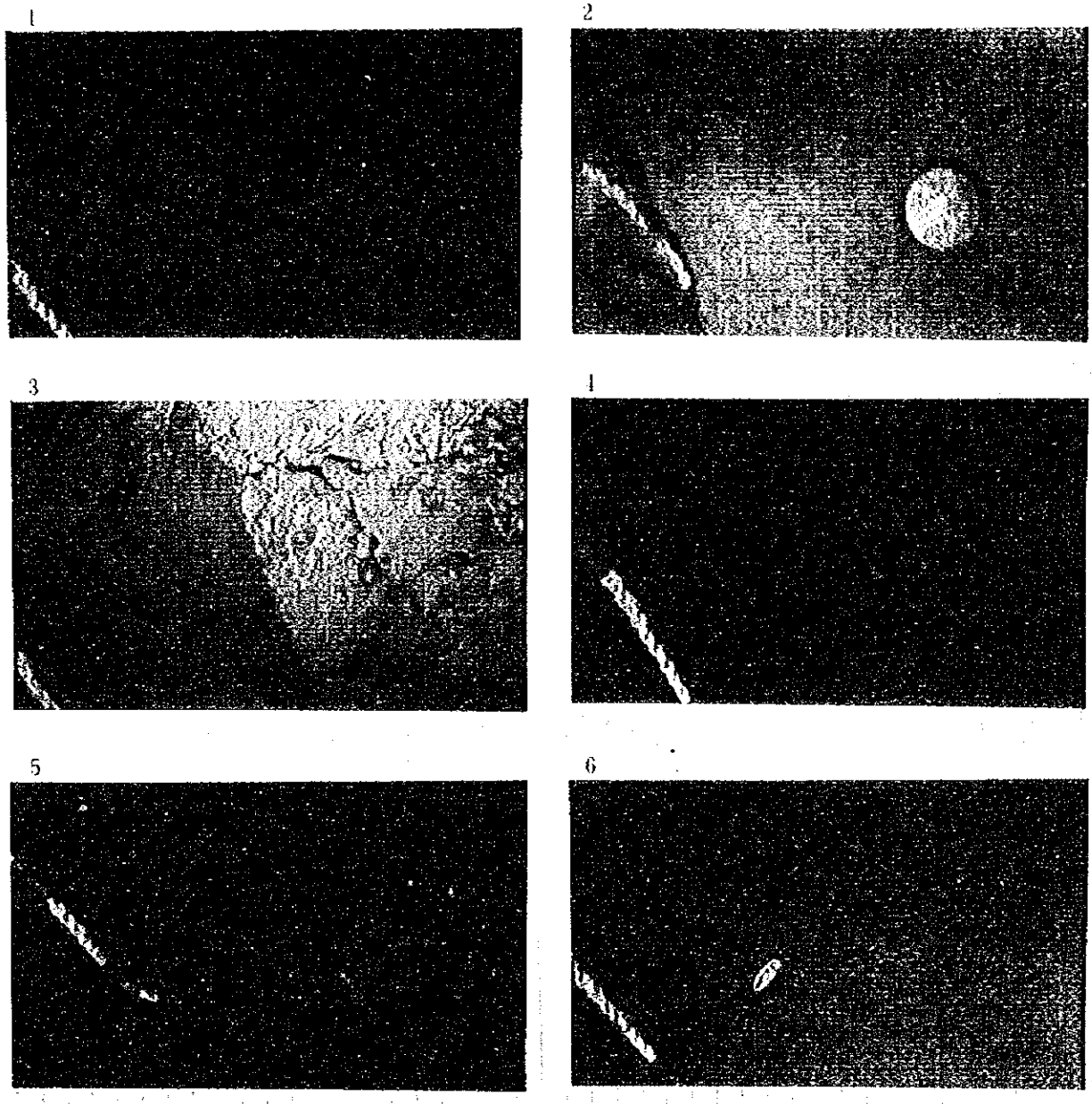

1. Shrimp (95SFDC10 21°23.68′S, 176°16.07′W, 1,781m)
2. Sea urchin (95SFDC08 21°24.78′S, 176°21.41′W, 2,079m)
3. Fish (95SFDC01 21°51.24′S, 176°30.04′W, 1,883m)
4. Fish *(Coryphaenoides acrolepis?)* (95SFDC10 21°24.07′S, 176°16.20′W, 2,075m)
5. Fish *(Bathysaurus?)* (95SFDC11 21°34.17′S, 176°19.73′W, 2,471m)
6. Shell *(Calyptogena magnifica?)* (95SFDC04 20°30.01′S, 176°11.04′W, 2,753m)

Fig. 4-3-1 (3) Photographs of FDC observation

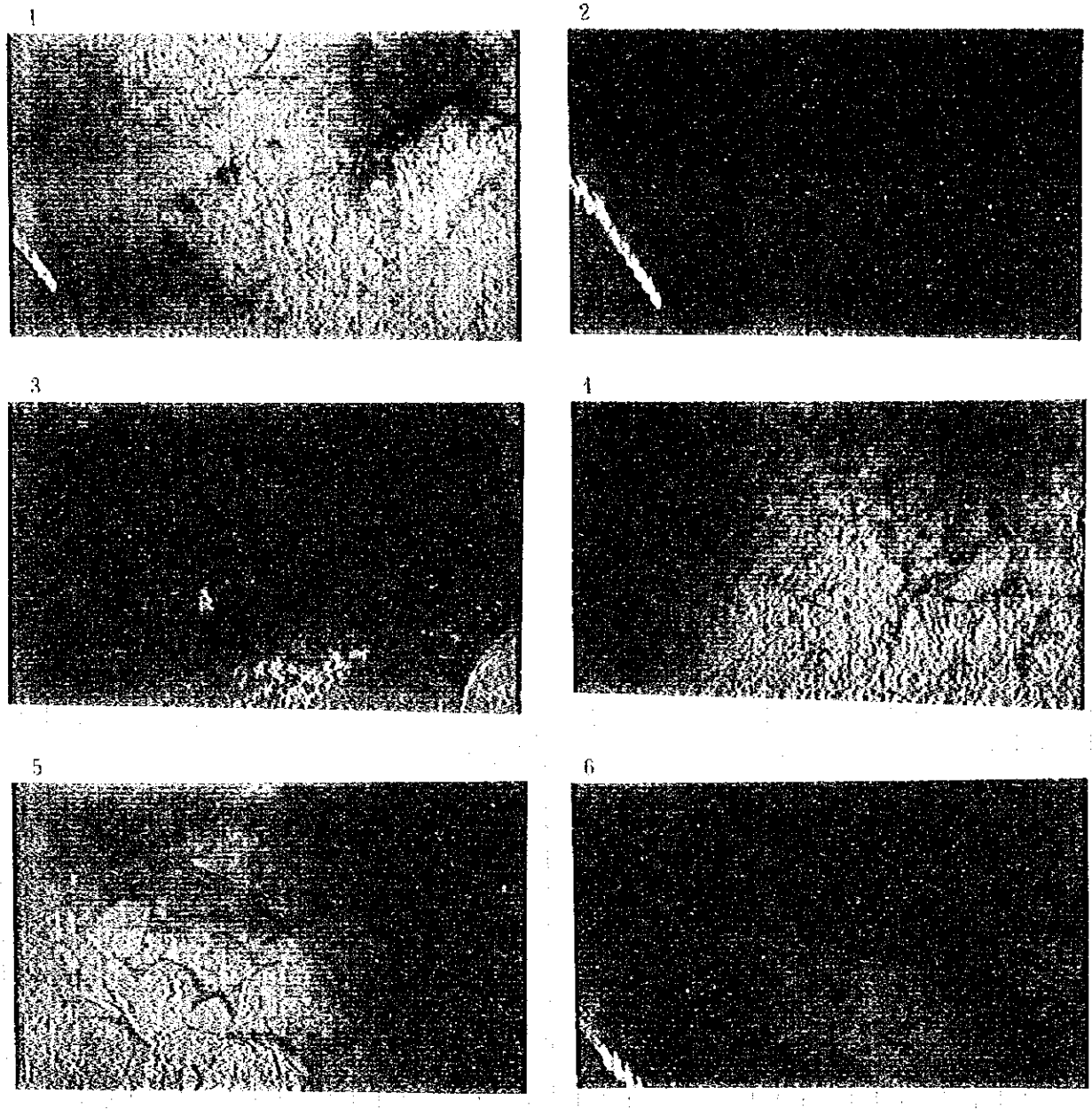

1. Mn and Fe oxides (95SFDC01 21°53.64′S, 176°31.16′W, 1,794m)
2. Mn oxides (95SFDC01 21°53.89′S, 176°31.33′W, 1,845m)
3. Fe oxides ans white materials (95SFDC01 21°54.99′S, 176°31.75′W, 1,895m)
4. Fe oxides (95SFDC01 21°56.16′S, 176°32.23′W, 1,836m)
5. White materials (95SFDC12 21°17.40′S, 176°21.17′W, 2,097m)
6. Reddish brown sediments (95SFDC12 21°17.32′S, 176°21.10′W, 2,074m)

Fig. 4-3-1 (4) Photographs of FDC observation

meters are developed and side walls of the cracks consist of pillow lava of 1 to 3 m in size. Pahoehoe lava were found in two places. On the topographic high in the north to the central part of the line, cliffs were developed.

Thin sediments totally cover lava, but the feature of lava underneath sediments can be observed. Thickness of sediments ranges from less than 1 cm to 10 cm. Although the line locates on the ridge and lava are very fresh, sediments are detected as this thickness. Thickness of sediments varies depending on the change of lava unit, not on the change of topography and lava formation.

As a sign of mineralization, yellow to brown substances which are assumed to be ferro-oxides were found in three places, and black manganese oxides in three places. The known ore deposit which is called White Church (manganese chimney, chimney of sulfides and barite, and mounds) was not recognized.

2) 95SFD02 (See Fig. 4-1-2 (2))

This line runs over the spreading center in Block TS-C, where the images suggesting a mound shaped topography were detected by the SSS survey. The line locates on the axial valley in the spreading center. Towing direction is NE to SW crossing the spreading center in low angle and the observation line length is 2.4 nautical miles.

Sediments are generally thick ranging from several cm to several 10 cm. Sediments are thick in the north of the line and little outcrops are few. Pillow lava and pillow breccia are prominent in the central to central-south of the line. On the summit of the plateau in the south most part, sheet lava are seen.

The open cracks are developed on whole line and range from several cm to several meters in width. Big scale cracks are more than 10 m in depth.

As a sign of mineralization, yellow-brown oxides and black manganese oxides were sporadically observed. One Munidopsis sp. was observed on the center.

3) 95SFDC03 (See Fig. 4-1-2 (2))

The objective of this line is to observe geological structures of the overlapping spreading center. The line crosses the bottom of the graben which is the spreading center in Block TS-C, and crosses the terrace where two spreading center join. Towing direction is NW to SE which crosses at right angles with the spreading center, and the observation line length is 2.4 nautical miles.

Near the terrace where two spreading center join thick sediments are seen. Fault cliff in the west of the terrace consists of pillow breccia and brecciated lava. In the center to the central west, pillow lava are widely observed.

Open cracks are seen on whole line, and range from several cm to several meters in width. Especially in the eastern part of the line on the terrace, many cracks are seen and some sediments exist even inside the crack. No ore indications are observed.

4) 95SFDC04 (See Fig. 4−1−2 (2))

This observation was carried out in the area where geothermal fluids are expected to erupt out as assumed on the depth profile of SSS results. The line locates in the axial valley of the spreading center. Towing direction is in SSW to NNE in parallel with the spreading center, and the observation line length is 2.4 nautical miles.

Sediments are abundant and thick over the whole line. In the south pillow breccia is widely seen, while in the central south pillow lava is dominant. Poor outcrops are seen in the north.

The open cracks are developed in the center. In the north, the muddiness of water and dead Calyptogena magnifica were observed, but neither water temperature anomaly nor ore indications were observed.

5) 95SFDC05 (See Fig. 4−1−2 (2))

This line was set in parallel with and about two nautical miles west of the line 95SFDC04. The line crosses the axial valley of the spreading center. Towing direction is SSW to NNE in parallel with the spreading center, and the observation line length is 1.4 nautical miles.

Sediments are widely seen with poor outcrop. Open cracks range from several 10 cm to 5 m in width. Side walls of the cracks consist of mainly pillow lava, pillow breccia, etc.

From the center to the south of the line, several hollows of sediments with a diameter of 20−50 cm were recognized, but the state under the hollows is unknown because of wide and thick covering of sediments. The muddiness of water was not seen on this line unlike the line 94SFDC04.

No ore indications are observed.

6) 95SFDC06 (See Fig. 4−1−2 (2))

This line was carried out in the area where the images suggesting a mound shape topography were recognized by the SSS survey. The line locates over the terrace in the eastern overlapping spreading center. Towing direction is from west to east at right angles with the spreading center, and the observation line length is 0.7 nautical miles.

Sediments are developed on the whole line, and pillow lava are sporadically seen on the sediments. There is a cliff consisting mainly of pillow breccia on the eastern end of the line. Sheet lava is

recognized on the foot of the cliff, and a white shrimp was found in the south. No ore indications are observed.

7) 95SFDC07 (See Fig. 4−1−2 (2))

This line was set on the overlapping spreading center in the south of Block TS−C in order to observe geological structures across the two spreading center. This line runs over the small knoll in the graben of the western spreading center, and crossing the terrace in the eastern spreading center. Towing direction is from west to east at right angles with the spreading center, and the observation line length is 4.7 nautical miles.

Sediments are widely seen from the west to the center of the line; while in the east sediments are poor with many outcrops. In the small knoll on the western spreading center, sediments are predominant, but many cliffs consisting of pillow lava are recognized. Sediments are abundant on the bottom of the graben in the center and the west of the terrace, and outcrops are few. The eastern outcrops consist of mainly pillow breccia, pillow lava and lobate lava.

On the terrace in the eastern half of the line, many open cracks are developed. The width of open cracks is generally large, ranging from 1 to several ten meters with an average of about 5 m. The cracks run in NNW−SSE to N−S direction in parallel with the spreading center. In the area where sediments are predominant, many hollows of sediments with a diameter of 20−50 cm are recognized. The graben in the center of the terrace has a width of 200 m and the cliffs on both sides have a height of over 50 m. Open cracks are also recognized on the summit of the small knoll in the west.

No ore indications are recognized.

8) 95SFDC08 (See Fig. 4−1−2 (3))

This observation was carried out in the area where the spreading ridge in the southern part of Block TS−D curves a little towards east in echelon shape. The line locates on the summit of the ridge crossing the spreading center. Towing direction is at right angles with the spreading center from west to east, and the observation line length is 3.4 nautical miles.

Thick sediments are predominant with local pillow lava on the margin of the spreading ridge summit in the eastern and the western part of the line. Outcrops are seen in the central spreading center, where pillow lava are predominant. Open cracks with a size of several meters are seen here, and cracks are many especially in the horst. In the west of the horst sheet lava and many collapsed pits of 3−5 meters deep and over 10 m in diameters are observed. In the eastern part where sediments are predominant, many small cracks of less than 1 meter in width are seen.

No ore indications are recognized.

9) 95SFDC09 (See Fig. 4−1−2 (4))

This line locates on the mountainous area with many small hills in the southwestern part of the Block TS−E, obliquely crossing the ridge which extends from the highest point of the seamount towards the north.

Towing direction is from NW to SE, and the observation line length is 6.3 nautical miles.

Sediments are not thick on the whole line, but rather thick on flat places or on gentle slopes. On the northwestern slope of the seamount in the northern part of the line, aa lava and pillow breccia are predominant, while in the central to the northern part, pillow lava and pillow breccia are predominant. Aa lava is predominant on the small hill in the southmost part of the line. Granules of black glass as the chilled margin are sporadically deposited like a line.

Steep cliffs corresponding to the topography are observed, but cracks are few.

As a sign of mineralization, black manganese oxides precipitation was confirmed on the small hill in the south of the line. Also, reddish brown sediments are observed on the northwestern slope of the seamount in the north.

10) 95SFDC10 (See Fig. 4−1−2 (3))

This line locates on the knoll chain which exists in the east of and in parallel with the spreading center in the southern part of the Block TS−D. The line crosses lengthwise the knoll chain and passes over two peaks of the knolls. Towing direction is from north to south along the knoll chain, and the observation line length is 3.3 nautical miles.

Sediments are thick on the whole line. The northern knoll consists of pillow lava and pillow breccia. Sediments are predominant in the southern knoll, and pillow breccia and aa lava are recognized. Outcrops are few in between two knolls on the center of the line, but aa lava and sheet lava are recognized.

As a sign of mineralization, yellowish brown precipitation of iron oxides is observed on the summit of the northern knoll, and rather many living things are observed from this point towards the north.

11) 95SFDC11 (See Fig. 4−1−2 (3))

This line locates on the small knoll in the east of the spreading center in the northern part of Block TS−E. The line crosses lengthwise the knoll and includes the flat place near the knoll. Towing direction is along the long axis of the knoll from NW to SE, and observation line length is 1.3 nautical miles.

Many cliffs consisting of pillow lava and pillow breccia are observed on the northwestern slope of the

knoll. On the gentle slope in the southeast of the knoll, abundant sediments, some pillow breccia and lobate lava are seen.

No outcrops are recognized on the flat place around the knoll, totally covered by sediments. A few gravels with a diameter of 10–30 cm are sporadically scattered on the surface of sediments.

No ore indications are found.

12) 95SFDC12 (See Fig. 4–1–2 (3))

This line was set in the northern end of the echelon shaped spreading center in the south of the Block TS–D. The line crosses the spreading center at slightly oblique angle. Towing direction is from SW to NE obliquely crossing the spreading center, and observation line length is 1.8 nautical miles.

Sediments are predominant in the southwestern part of the line, and some aa lava and lobate lava are recognized. Outcrops of pillow lava and pillow breccia are seen in the central to northeastern part of the line.

Open cracks range from 1 m to 5 m in width.

As a sign of mineralization, white precipitations (alteration?) were observed on the surface of pillow lava in two places in the central south, of which reddish brown precipitation was also observed in one place.

13) 95SFDC13 (See Fig. 4–1–2 (3))

This line was set in almost flat place on the summit of the spreading ridge in Block TS–D. The line crosses the spreading center which forms a small horst. Towing direction is perpendicular to the spreading center from WSW to ENE, and the observation line length is 2.1 nautical miles.

In the west of the line, sediments are predominant, and the cliffs consist of pillow lava. Outcrops are seen on the center, where pillow lava is predominant with locally pahoehoe lava, sheet lava and lobate lava. In the eastern part, pillow lava, aa lava, lobate lava are confirmed with rather abundant sediments compared with the central part.

Cliffs and many cracks are few on the whole line. In the center, open cracks are observed on sheet lava and collapsed pits are seen on lobate lava.

As a sign of mineralization, white surface rocks were observed on the western end of the line.

4-4 Sampling

(1) LC

The object of sampling by LC is to study geological characteristics and conditions by collecting sediments of the sea floor, where the hydrothermal ore is expected to exist, and to provide the information for geochemical survey. In short, a direct object is to find out ore deposits and ore indications, and an indirect object is to select geochemical anomaly. Sampling locations are shown in Fig. 4-1-2 (1)-(4) and representative photos of sampling are shown in Fig. 4-4- 1 (1),(2). LC core columnar chart, list of sampling results (Data of sampling locations, etc.) and list of specimen for analysis and identification are shown in Appendix Fig. 2, Appendix Table 2 and Appendix Table 4, respectively.

Sampling locations mainly concentrated in the spreading center of the basin where the hydrothermal activity is expected, but three areas are located according to the purpose of sampling. In Block TS-A, samplings were made with the object of collecting sediments in the remote area from the spreading center where little possibility of hydrothermal activity is expected. While in Block TS-B and Block TS-C, samplings were made with the object of collecting sediments on and near the spreading center, where MBES acoustic reflection image suggested the distribution of sediments. In Block TS-D, sampling were made in order to study geochemical data variation near the spreading center on the base line crossing the spreading center at right angles.

The numbers of sampling stations are 1 in Block TS-A, 8 in Block TS-B, 8 in Block TS-C, 14 in Block TS-D, totaling 31 stations, in which sediments were collected at 19 stations, while no sediment samples were collected at 3 stations in Block TS-B, 4 in Block TS-C, 5 in Block TS-D, totaling 12 stations. In some stations of no sediments collected, however, basaltic lava fragments or pumice were collected.

Columnar cores were split into two portions in depth direction, and after the descriptions the half was appropriated to geochemical analysis and the remaining portion were preserved.

Color tones of the sediments were classified by thin color tones based on MUNSELL SOIL COLOR CHARTS. Color tones of the sediments in this area are mainly composed of 10YR series (brownish series) and 5Y series (olive and gray series). Grain size is mainly composed of silt and little clay, and partly sand layers are interbedded. The main composition of sediments is fine grain pyroclastics with volcanic ash characteristically interbedded. Followings are the summary for each Block;

1) Block TS-A

Sampling was made at one station about 25 km east of the spreading center as shown in Fig. 4-1-2 (1). This station is most remote from the spreading center among all sampling stations and it is

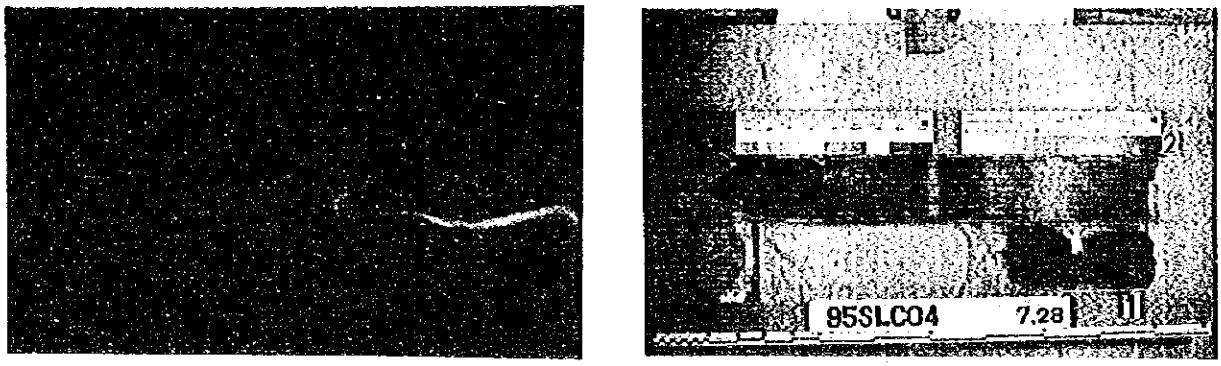

1. 95SLC04 : Sea-floor (left), section of sediments core (right)
Sediments in the ridge adjoining the spreading graben

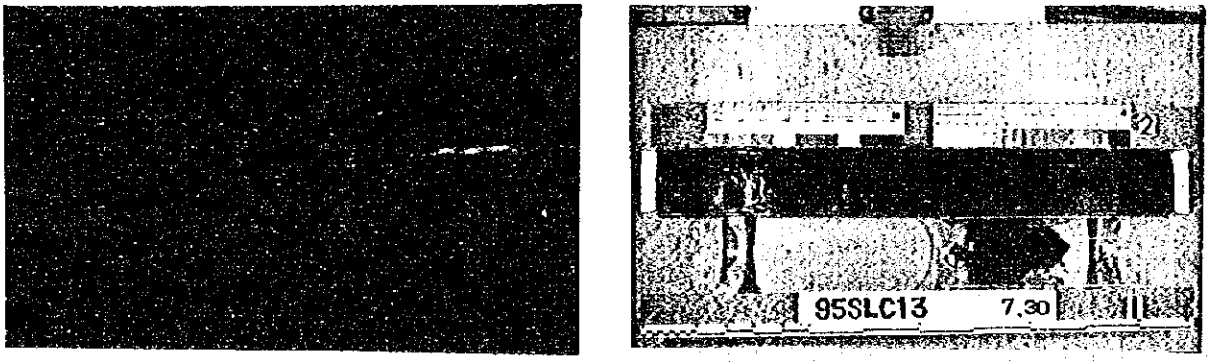

2. 95SLC13 : Sea-floor (left), section of sediments core (right)
Sediments in the graben distant from the spreading graben

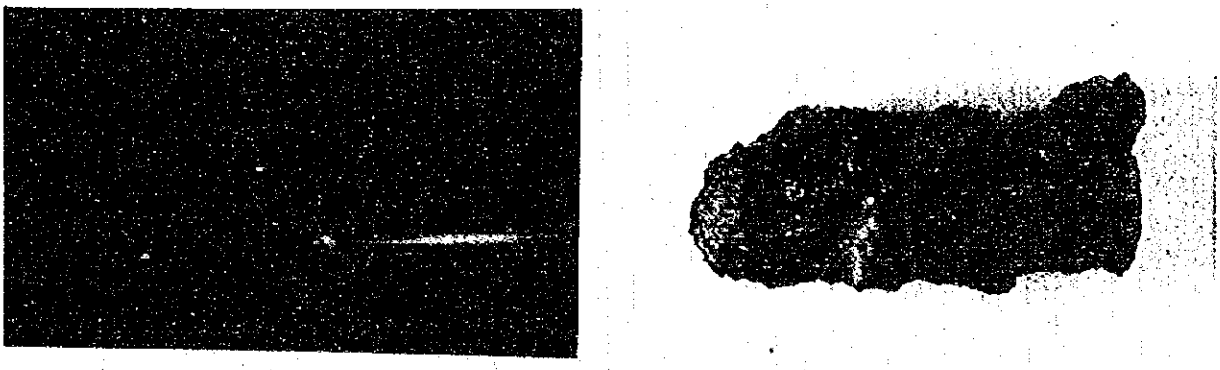

3. 95SLC12 : Sea-floor (left), section of rock fragment (right)
Outcrop in the ridge distant from the spreading graben
Very porous basalt with weak pyrite dissemination

Fig. 4-4-1 (1) Photographs of LC sampling

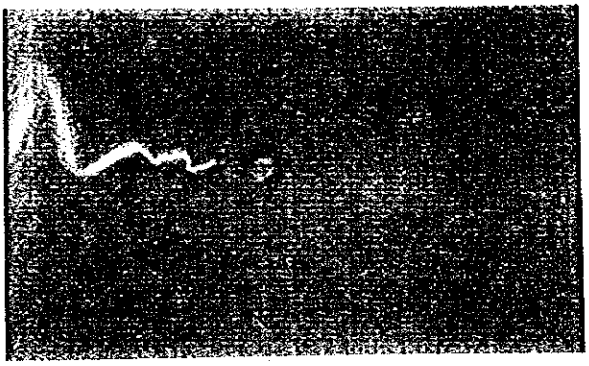

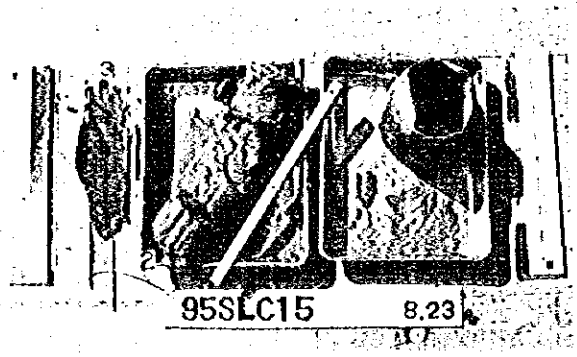

4. 95SLC15 : Sea-floor (left), sediments core (right)
   Sediments in the spreading axis
   Bedrock lies under the sediments bacause of the bit deformation

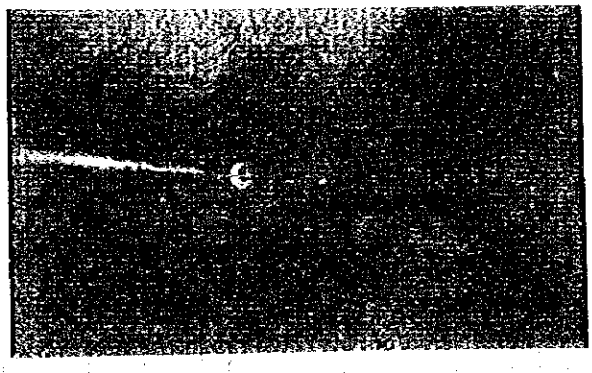

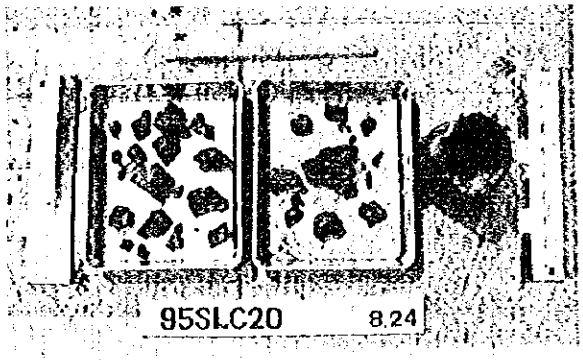

5. 95SLC20 : Sea-floor (left), rock fragments (right)
   Bedrock in the spreading axis
   Basalt with weak pyrite dissemination and black glass of chilled margin

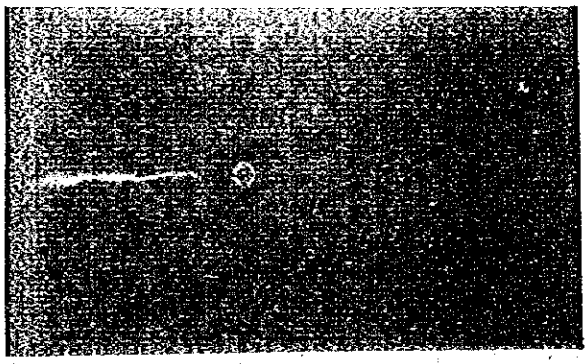

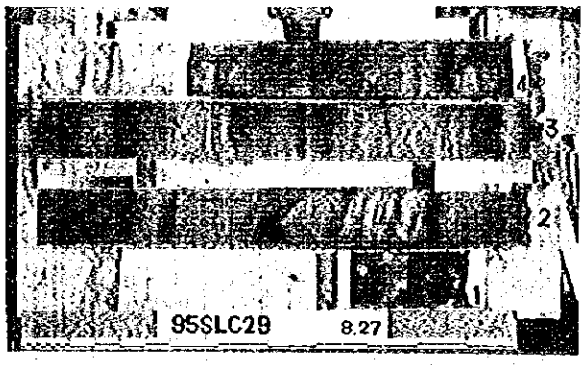

6. 95SLC29 : Sea-floor (left), section of sediments core (right)
   Sediments in the ridge far from the spreading axis
   The longest sediments core in the LC sampling

Fig. 4-4-1 (2) Photographs of LC sampling

assumed that little influence of hydrothermal activities exist in the sediments.

The length of columnar core 95SLC27 is 215 centimeters, and brown mud and olive mud are dominant, in which there are 16 layers of black ash or sand interbedded with a thickness of about 0.5 to 1 centimeter. These layers are dense in the upper part and the distance of two layers becomes wide towards the bottom. Black volcanic ash consists of black volcanic glass, with partly basaltic fragments and pumice. At the depth of 105 to 115 centimeters and 150 to 180 centimeters of the core, pale gray fine acidic volcanic ashes are interbedded.

Calcareous foraminifera shells are recognized in all formation. Water content is low in general.

2) Block TS−B

In this block, the number of sampling station is eight; 3 stations in the graben of the spreading center, 4 stations in the east of the graben, and one in a small horst. No sediments or rocks were collected at three stations on 95SLC23 − 95SLC25 because the sea floor was outcrop. Both 95SLC26, 95SLC28 and 95SLC30, 95SLC31 locate in the same small graben, while 95SLC29 locates in a small horst between the small grabens. The core collected at 95SLC29 is the longest size of 285 centimeters among all cores.

Sediments consisting mainly of brown mud (partly olive mud) are predominant in this block, among which 8 − 19 layers of black ash or the same volcanic sand are interbedded. Except 95SLC29, 2 to 3 layers of black to gray volcanic ash are interbeded with a thickness of 10 to 30 centimeters and the lower part of the layer gradually change to black volcanic ash in most case. At 95SLC26 and 95SLC28, nearest to the spreading center, the thickest volcanic ash or the same volcanic sand among all of sampling sites are interbedded.

At 95SLC29, alternating bed of brown and reddish brown mud are predominant, interbeded irregularly by 1 centimeter thick volcanic sand. Pale gray siliceous wooz exists at the depth of 100 to 105 centimeters, and the same wooz is also recognized at 95SLC30.

3) Block TS−C

Eight samplings were made mainly in the east of the graben of the spreading center, as shown in Fig. 4−1−2 (2). No sediments were collected at four stations ; 95SLC16, 95SLC18, 95SLC20 and 95SLC22, but basaltic lava was taken at 95SLC20. Sediments were collected at 95SLC15, 95SLC17 and 95SLC21, but the tip of the LC bit was deformed.

Sediments are mainly brown mud, with one to four layers of volcanic ash or the same sand interbeded. The thickness of these layers ranges from 2 to 5 centimeters.

Two layers of volcanic sands are seen at 95SLC17, showing the normal grading changing from fine to

coarse grain in the layer. Foraminifera is abundant in the bottom part of these sand layers.

In general, volcanic ash or sand layers are fewer in this block compared with Block TS−A and TS−B, but the characteristic point is that one layer is thicker than that of the other blocks.

4) Block TS−D

A base line was set crossing the spreading ridge at right angles as its center. Fourteen samplings were made with the object of studying the change of geochemical characteristics near the spreading center. Topographic features of the sampling area are the alternation of the small scale horst and graven with a short cycle, which are parallel with the spreading center running in NNE−SSW direction. Sampling locations are selected to locate on the small scale horst and graven in 14 stations in total, 2 in a small trench on the spreading center, 7 in the east and 5 in the west of the spreading center as shown in Fig. 4−1−2 (3).

The columnar cores were collected at nine stations and their lengths are 55 to 110 centimeters. No sediments were collected at five stations; 95SLC01 and 95SLC02 on the spreading center, 95SLC06 in the eastern side, 9SLC11 and 95SLC12 in the western side, among which small rock fragments were collected at two stations.

The surfaces of sediments are mostly brown mud and it has a general tendency to become olive mud in dominant towards the bottom. Several to over ten layers of volcanic ash and sand are interbeded. Volcanic ash consists of black volcanic glass rarely accompanied by basaltic rock fragments. This layer shows the typical grading with abundant foraminifera. Pumice pebbles are partly included in brown mud and there is the tendency that bigger pumices with a diameter of 2 to 5 centimeters exist in the upper part of brown mud layer just under the ash layer.

As a local characteristic, volcanic ash is dominant in the east of the spreading center and volcanic sands in the west. Subrounded pumice pebbles and basaltic lava fragments were collected at 95SLC01 and 95SLC12, respectively. Little amount of sulfides (pyrite) was recognized in basaltic lava fragments collected at 95SLC12.

(2) FPG

The object of sampling by FPG is to collect rocks or ores. In the southernmost part of the area (Block TS−E), sampling was carried out in three stations; the spreading ridge, seamount which knolls gather to make, and knoll chain in the east of the spreading center, which form a characteristic topographic feature. Sampling locations are shown in Fig. 4−1−2 (4) and typical sampling photos are shown in Fig. 4−4−2. List of sampling results such as sampling locations, etc. is shown in Appendix Table 2.

Sampling results at each station are summarized as follows;

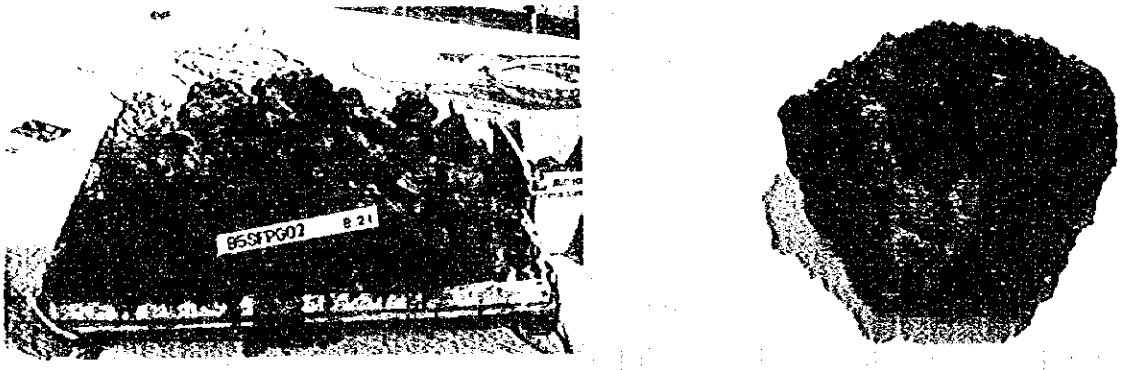

1. 95SFPG02 : The whole samples (left), basalt lava (right)
Almost rocks are slaggy aa lava and
some are pahochoe-like lava (right)

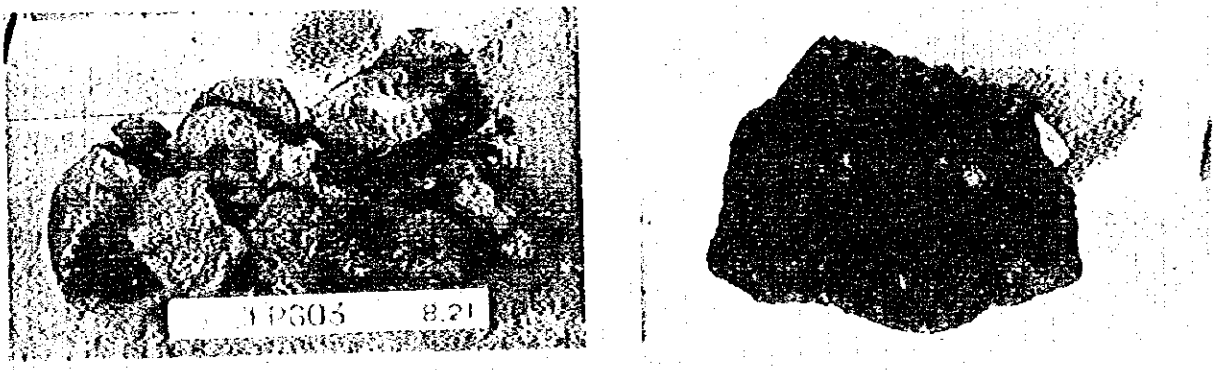

2. 95SFPG03 : The whole samples (left), basalt lava (right)
Rocks are pillow lava with abundant radial joints
Lava surfaces are brown by oxidization

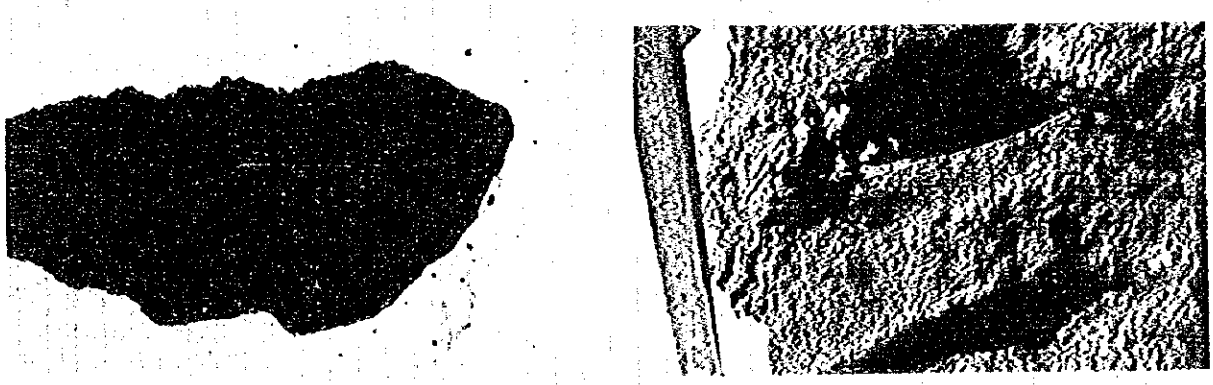

3. 95SFPG01 : Basalt lava (left), close-up of the sectional surface (right)
Pillow lava has a bedded structure near the surface
Pillow lava is very porous and has some big cavities

Fig. 4-4-2 Photographs of FPG Sampling

1) 95SFPG01 (See Fig. 4−1−2 (4))

Sampling was made in the seamount which forms a group of knolls in the west of the spreading center. Samples are basaltic pillow lava as well as brown mud.

Basalt has radial joints and the fresh part shows greenish dark gray, partially with brown to yellowish brown weathering. In the surface of lava, chilled margin consisting of dark glass is formed with a thickness of about 4 millimeters. The layers of glassy chilled margin in parallel with the surface are recognized at the interval of about 2 centimeters. The inside of lava is porous with abundant gas cavities and the diameter of gas cavity is increasing towards the center. An average diameter of gas cavity is 2 to 3 millimeters, but the very large gas cavity of 3 by 10 centimeters is also recognized. Phenocrysts are peridotite with a maximum of 3 millimeters and an average of 1 millimeter in size.

2) 95SFPG02 (See Fig. 4−1−2 (4))

Sampling was made on the summit of the spreading ridge. Samples are basaltic aa lava and a little amount of porous pumice and brown muddy substances.

Most of basalt is irregular shaped and slaggy aa lava. Some are pahoehoe−like lava with meander ripple marks of several millimeters in width. Basalt is very fragile and easily broken.

The fresh part is black to greenish dark gray and reddish brown oxidized part is much. The surface of lava is black glassy chilled margin with a thickness of about one millimeter, and the inside is porous with abundant gas cavities. The diameter of cavity is about one millimeter in average, which is smaller than 95SFPG01. Spindle shaped cavity is also recognized. Peridotite is recognized as phenocryst.

3) 95SFPG03 (See Fig. 4−1−2 (4))

Sampling was made on the knoll chain in the east of the spreading center.

Samples are basaltic pillow lava, which show radial joint. The surface of lava is compact black glass with a thickness of about one centimeter. Several centimeters from the surface are greenish gray, to which depth is chilled margin. The surface of glass layer is reddish brown due to oxidation, and the fresh inside is greenish dark gray to black and generally porous except glass part. The number of cavities increases towards inside and cavities are abundant especially within 10 centimeters from the surface. The diameter of cavity is about 2 millimeters and its shape is circle or ellipse. Peridotite with a maximum diameter of 2 millimeters and an average diameter of 0.7 millimeters are recognized as phenocryst.

(3) CB

Sampling by CB was carried out near the spreading center with the object of collecting rocks. The numbers of sampling stations are 11 in total; 5 in Block TS-B, 3 in Block TS-C and 3 in Block TS-D. The towing direction of CB is from west to east or from northwest to southeast taking into consideration the wind and current directions. Therefore, west fallen cliffs or west dipped slopes generally become the target of sampling. Location maps of sampling are shown in Fig. 4-1-2(1)-(3), and the representative sampling photos are shown in Fig. 4-4-3. List of sampling results such as sampling location data etc. is shown in Appendix Table 2.

Most of samples are basaltic lava with a little amount of pumice and brown muddy substances.

Followings are the summary of sampling results in each block.

1) Block TS-B

Five samplings were carried out as shown in Fig. 4-1-2 (1); 2 stations on the eastern cliff of the graben which is a margin of the spreading center, 2 stations on the western slope of horst in the east of the spreading center and 1 station on the western slope of the knoll chain about 35 kilometers away from the spreading center.

Only basaltic lava were abundantly collected around the spreading center, while pumices as well as basaltic lava were collected in the east of the spreading center. The quantity of pumice increases towards east and basaltic lava decreases on the contrary.

At 95SCB07 near the spreading center, pillow lava, pahoehoe lava and sheet lava were collected. Pahoehoe lava shows thin sheet with less than ten centimeters thickness and has black glassy chilled margin on both sides of the sheet. One side shows a characteristic structure with many duplicated ropy folds of about one centimeter diameter. The other side has numerous small projections coated by manganese oxides. Sheet lava also shows thin sheet with black glassy chilled margins on both sides. One side looks like a sharkskin surface and the other side with numerous projections coated by manganese oxides.

At 95SCB08 near the spreading center, pillow lava was collected. The surface of pillow lava is black chilled margin with a thickness of about 5 millimeters. The inside of lava is porous and the fresh part showing dark gray color. The surface of lava and cracks are brown due to oxidation.

Basaltic lava collected at 3 stations in the east of the spreading center are not as much as in the spreading center and many subrounded pumices are collected. As a comparative quantity of basaltic lava and pumice basaltic lava is less in the east. The lava form is indistinct because the size of lava is small. Basalt is oxidized and coated by manganese oxides with the tendency that the oxidation and manganese coating are stronger towards east. Some of basalt are compact and dark gray aphyric and

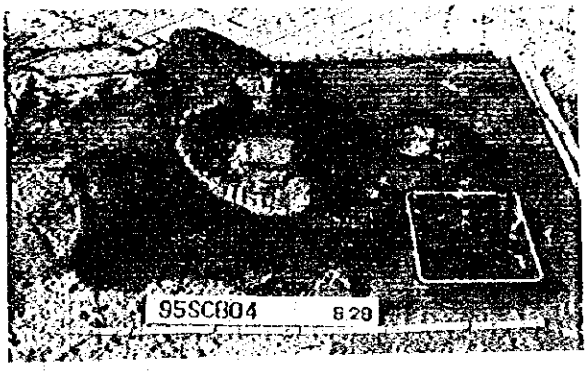

1. 95SCB04
The whole samples of pillow lavas
One of pillow lava has a big tubular cavity in the central part

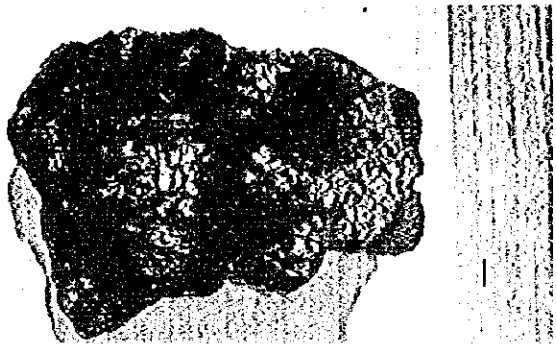

2. 95SCB05
Surface of pillow lava
The surface is black glass of chilled margin

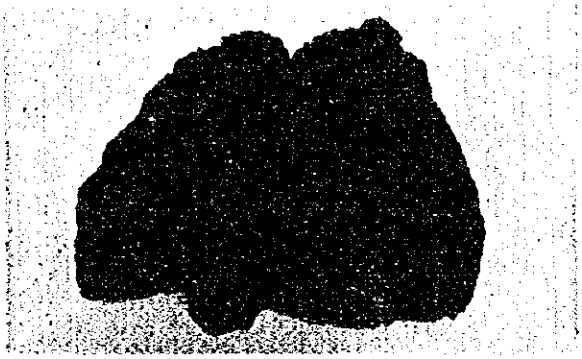

3. 95SCB03
Sectional surface of pillow lava
Thin bed of black glass(chilled margin) exists inside the lava

4. 95SCB06
Sectional surface of pillow lava
Thin Mn oxides cover the rock

5. 95SCB07
Surface of sheeted lava
The surface is black glass and has a lot of small knobs

6. 95SCB07
Surface of pahoehoe lava
Ropy structure on the surface is very distinctive

Fig. 4-4-3 Photographs of CB sampling

some are greenish gray and porous. Cavities are mostly ellipse with a maximum diameter about 5 millimeters. Some of pumice are pale gray and porous, and some are gray and glossy with bedded and fibrous texture.

2) Block TS--C

Three samplings were made as shown in Fig. 4--1--2 (2); two stations on the western slope of the topographic high in the graben of the spreading center and one station at the eastern cliff of the graben.

Basaltic pillow lava were collected at three stations. Cylindrical pillow lava was collected at 95SCB04 on the spreading center. The diameter of cylinder is about 35 centimeters and the core forms a cavity with a diameter of 10 centimeters.

The surface of lava is black glassy chilled margin with a thickness of about 1 cm, and the inside is black and compact chilled layer, and further inside is dark gray to greenish dark gray fresh lava. Very coarse phenocrysts of feldspar are abundant in the whole part including marginal glass. The maximum length of phenocryst is 10 millimeters with an average of 5 millimeters.

No other basaltic lava contains such a large phenocryst of feldspar, so that it is considered to be a zenocryst.

Pillow lava collected at 95SCB05 on the spreading center has several black glass layers with a thickness of 2 – 3 millimeters even in the inside of lava. In between the layers there are greenish gray and fresh nonporphyritic part. The surface of lava is coated by manganese oxides.

Pillow lava collected at 95SCB06 in the east of the spreading center are more porous than the above mentioned two samples. The surface is black glass with a thickness of about 4 millimeters, and fresh part inside is dark gray. The shape of cavities is circle to ellipse and the average diameter is about 2 millimeters. The surface of lava is covered by manganese oxides.

3) Block TS--D

A little amount of pyrite was found in basaltic lava collected by LC sampling on the horst in the west of the spreading center. Therefore, two samplings were carried out on the western foot and the western slope of the horst. In addition to one sampling in the spreading ridge, the total three samplings were made as shown in Fig. 4--1--2 (3).

At 95SCB03 on the spreading center, basaltic pillow lava was collected. The surface of lava is very thick black chilled margin with a maximum thickness of 7 centimeters. The inner fresh portion shows greenish gray color. The maximum diameter of cavity is about 1 centimeter with an average of 3 millimeter. The part around the crack is yellowish brown due to oxidation. A few pumices were also

collected.

At 95SCB01 and 95SCB02 in the west of the spreading center, no basalt but pumice pebbles were only collected. Pumice is very porous and the surface is brown to greenish gray. Pebbles are subrounded and the maximum diameter is 15 centimeters.

4-5 Survey Results

(1) Geology and Rock Facies

The basement rock of the survey area is basaltic lava and lava forms are pillow, breccia, aa, sheet, pahoehoe, etc.

No other rocks except basalt were collected. Sediments covering the basement rock are unconsolidated mud which consists mainly of volcanic glass with poor clay. Muddy sediments will be mentioned later.

In general, rocks well outcrop and sediments are poor in the spreading center. Steep slopes consist of brecciated lava, pillow breccia and aa lava in most cases, while sheet or pahoehoe lava are seen in flat places. On the fault cliff near the spreading center, pillow lava are seen on the summit of the cliff and brecciated lava are distributed in the middle to the lower part of the cliff. On the slope of horst and knoll brecciated lava and pillow lava are dominant, and near the summit pillow lava and lobeit lava are predominant.

Lava with columnar joint or platy joint are rarely found. This means that there is no thick lava flow with high viscosity which cause joints to be developed. The intrusive rock which forms a linear and almost vertical board is locally found.

In the northern part of the survey area, pillow lava, pillow breccia and brecciated lava are predominant, and open cracks caused by the spreading are found wholely. The width of the open cracks ranges from several centimeters to several 10 meters order in wide variation. Most of the cracks extend in parallel with the spreading center. Collapsed pits are seen in several places.

In the southern part of the area, the spreading ridge mainly consists of aa lava and brecciated lava. Pillow lava are also seen in many places. These mostly make a steep slope or cliff unlike the northern area, which suggest the higher viscosity of lava.

Lava are generally porous with abundant gas cavities which show circle, ellipse, tube or irregular shapes. The quantity of phenocryst ranges from non or poor to rich. The examples of rich phenocryst are as follows; 95SFPG01 (coarse phenocryst of olivine), 95SCB04 (coarse phenocryst of rich feldspar and fine phenocryst of poor olivine). Judging from the fact that some of coarse grained olivine are xenocrysts (J.W.Hawkins, 1985), feldspars of the latter must be the same.

All lava have the chilled margin. The thickness of chilled margins ranges widely from several millimeters to several centimeters. The surface crust is black glass with various thicknesses.

Followings are the forms of basalt lava in different types.

1) Pillow lava

Pillow lava is the most common lava in this area.

The sectional shape of lava is mostly round to oval and the external form is pillow to tube. The shape of lava is actually very variable as follows;

Elongated tube, curved tube, irregular curved tube, barrel, gourd, a group of several knots, ball, rugby ball, branch shape, etc. On the slope such tube lava hang down.

On the surface of lava, cooling cracks like parallel stripes, tortoiseshells and grid lines are common. The cooling radial joints are also abundant. The surface part of lava is fine grained and glassy with the chilled margin, and the crust part is black glass. In general the glass crust is compact and the inside is porous with many gas cavities.

In the section of lava, the banded structure like an annual ring in parallel with the surface is occasionally observed. This is formed by the repeats that after the surface of lava flow is cooled and becomes a solid, the inside is still molten and mobile, and then its surface is cooled again. The lava collected at 95SCB04 has a big cavity in the center.

After cooling, pillow lava is broken into breccia by the movement of new lava flow, so that pillow breccia is formed.

2) Brecciated lava

This is lava blocks brecciated and piled after eruption and autobrecciated lava showing a brecciated structure. There are two types of brecciated lava; one is developing upward faster than lateral flow, and the other is formed on the edge of lava flow. The occurrence of the former one causes the abundant supply of lava with high viscosity. The diameter of breccia is mostly several ten centimeters.

No typical breccia samples were collected, but there is a tendency that the development of chilled margin is not so stronger than the other lava.

3) Aa lava (Slag lava)

Aa lava is irregular shape with abundant gas cavities. The surface is very rugged with many projections and wrinkles by the cooling and flow movement. This aa lava is second dominant after

pillow lava.

4) Sheet lava

Surface of sheet lava is flat and plane. This is a pattern of pahoehoe lava or a kind of massive lava. Flow structures seen to be developed under FDC observation.

Sheet lava collected with pahoehoe lava at 95SCB07 are thin sheets with the thickness of several centimeters to 10 centimeters, showing platy joint. Both surfaces have a chilled margin with many small projections.

5) Pahoehoe lava (Ropy lava)

The parallel ropy wrinkles on the lava surface are characteristic.

These are observed in the track line of 95SFDC13 and samples were collected at 95SCB07. The thickness of lava is about 4 centimeters and ropy wrinkles consist of chilled glass.

(2) Muddy Sediments

Characteristics of sediments collected by LC are as follows; many ash layers are interbedded, pyroclastics are abundant with less clay, and microfossils are found in all layers.

There are two types of volcanic ash; one is black to dark gray, very coarse to fine grained ash, and another is pale gray, fine grained ash. Sediments other than ash are silt consisting mainly of pyroclastics, of which color is separated into brown group and olive group. Brown group which suggests the oxidation decreases from the surface to the bottom, while olive group which suggests the reduced environment increases. Microfossils observed with naked eyes mainly consist of foraminifera of less than one millimeter. Shells with several millimeters are rarely found. Little amount of fine grain sulfide is confirmed in muddy sediments at several places in the spreading center.

The thickness of sediments is less than several ten centimeters in the spreading center, and it tends to increase away from the spreading center.

At 95SLC21, the eastern edge of the graben in the spreading center, the thickness of sediments is about one meter, while at 95SLC29, 10 kilometers east away from the spreading center, it is over 3 meters.

Black ash is erupted out from volcanic activities of knolls in and around the spreading center and submarine volcanoes in the Tonga Ridge. The thickness of ash and grain size vary according to the location. This is considered to be due to the topography and the current, but in general, grain size becomes coarse and the number of ash layer increases as the location becomes close to the spreading

center. The thickness of ash increases in the valley part, but thick ash is also recognized at some places in the east of the spreading center. This is caused by the fact that knoll chains and submarine volcanoes with the new volcanic activity exist in the east of the spreading center. Volcanic ash layer shows a normal grading and includes more muddy substances towards the upper. Mostly in the bottom of the ash layer, many foraminifera occur. Basaltic fragments and pumice are partly included.

Pale gray volcanic ash is the product of an island arc type acidic volcanic activities in the Tonga Ridge. This ash consists of semitransparent volcanic glass, which shows fine and homogeneous grain size in comparison with black ash.

As mentioned above, sediments mainly consist of pyroclastic materials, with many volcanic ash layers interbedded, which indicate the considerable supply of volcanic pyroclastics from island arc, submarine volcanoes and the spreading center.

(3) Ore Indications

Ore indications confirmed by the FDC survey are only precipitations of black manganese oxides and yellowish brown iron oxides, reddish brown and white sediments. The distributions of the above are very local and the scale of the distribution is very small. Total ore indications are found only in eleven places.

By the LC sampling, little quantity of sulfides is confirmed in non altered basalt fragments in two places, and small amount of very fine grained sulfides is also found in muddy sediments in several layers.

By the FPG and CB sampling, no ore indications are confirmed.

As mentioned above, no characteristic signs for hydrothermal ore deposits are found such as massive sulfides, chimney, altered clay, hydrothermal living things, etc.

Ore indications confirmed in each place are as follows;

1) 95SLC12 (See Fig. 4--1--2 (3))

A small amount of sulfide dissemination is confirmed in basaltic pillow lava fragments collected on the horst about four kilometers west of the spreading center in Block TS--D. Basalt is not altered with naked eyes and no other alteration than sulfides is confirmed.

Sulfides are identified to be pyrite by the microscopic observation. The grain size of pyrite is less than one millimeter and the quantity is small.

2) 95SLC20 (See Fig. 4-1-2 (2))

A small amount of sulfide dissemination is confirmed in pillow lava fragments collected on the topographic high in the spreading center in Block TS-C. Basalt is not altered with naked eyes and no alteration but sulfides are confirmed.

Sulfides are identified to be pyrite by the microscopic observation. Pyrite is disseminated along the fractures with a grain size of 1 to 2 millimeter and the quantity is small.

3) 95SFDC01 (See Fig. 4-1-2 (4))

Precipitations of manganese oxides and iron oxides are observed on the FDC track line along the spreading ridge in Block TS-E.

Black manganese oxides are found in three places. Some are precipitated around the vent of hydrothermal eruption in the sediments and others stick to the rock surface. The latter must have produced due to the direct contact of hydrothermal fluid with rock near the erupting vent like the former.

Yellow-yellowish brown-brown iron oxides are found in three places. Some are precipitated along the fracture or deposited in the vicinity, and others are precipitated in the inner wall of a small collapse pit. In the latter place, white materials are observed inside the pit, but details are unknown.

4) 95SFDC02 (See Fig. 4-1-2 (2))

Precipitations of manganese oxides and iron oxides are observed on the FDC track line in the graben of the spreading center in Block TS-C.

Black manganese oxides and yellowish brown iron oxides are dispersedly observed within the area of about 100 meters. These are deposited around the vent found in the sediments or along the outside of gravels.

5) 95SFDC09 (See Fig. 4-1-2 (4))

Black materials are observed on the FDC track line crossing obliquely the seamount in the west of the spreading center in Block TS-E. Black materials are assumed to be the stick of manganese oxides, but no other detail information is collected.

6) 95SFDC10 (See Fig. 4-1-2 (3))

Brown and white materials are observed at one place on the FDC track line crossing the knoll in the

east of the spreading center in Block TS-D. Yellowish brown iron oxides are precipitated on the fracture in the sediments or along the outside of gravels.

7) 95SFDC12 (See Fig. 4-1-2 (3))

Brown and white materials are found on the FDC track line crossing the spreading center in Block TS-D. White ones sticking thinly to the rock surface are found in two places, in one of which brown oxidation on rock surface is also observed.

8) 95SFDC13 (See Fig. 4-1-2 (3))

White materials are found on the FDC track line crossing the spreading center in Block TS-D. These are white alteration on rock surface, but details are unknown.

(4) Temperature Anomalies

On-line measurement of water temperature by CTD was performed simultaneously with the FDC survey for 13 FDC track lines. As the conditions of measurement, towing speed is 1 - 1.5 knots, and interval of data acquisition is 5 s (sampling intervals about 3 - 4 m).

Considering variations of background values of temperature and depth along each track line, values regarded as anomalies were determined. Lists of water temperature anomaly are shown in Table 4-5-1, and temperature - CTD depth profiles are shown in Fig. 4-5-1 (1)-(3).

A few temperature anomalies were detected on 6 FDC track lines. Temperature anomalies change in a range of 0.010 to 0.050 ℃ .

In comparison with FDC observation results, locations of temperature anomalies mostly correspond with the locations where cliffs, fissures and cracks are identified. However, no living things or precipitations which indicate hydrothermal activities were observed. Only on 95SFDC01 track line, gossan of rock and iron oxides are found, and on track lines of 95SFDC09 and 95SFDC10, manganese oxides coatings and yellow precipitations are observed, respectively, of which temperature anomalies may suggest indication of hydrothermal activities.

Table 4-5-1 List of temperature anomalies

Line No.	Temperature Anomalies No.	Temperature (℃)	Depth (m)	Date/Time (GMT)	Position	FDC Results of Observation
FDC-01	①	2.496 (+0.015)	1,763	08/08 22:15:05	21°52.851'S 176°30.837'W	Cliff
	②	2.501 (+0.016)	1,790	08/08 23:00:55	21°53.649'S 176°31.174'W	Fissure Fe-oxides
	③	2.547 (+0.070)	1,870	08/09 01:14:05	21°55.928'S 176°32.158'W	Sheeted lava
FDC-05	①	2.342 (+0.013)	2,743	08/14 00:59:35	20°29.900'S 176°11.144'W	Fissure
	②	2.348 (+0.021)	2,726	08/14 01:21:35	20°29.529'S 176°11.044'W	Cliff
FDC-07	①	2.326 (+0.013)	2,445	08/15 00:14:55	20°32.544'S 176°12.199'W	Fissure
	②	2.329 (+0.010)	2,610	08/15 01:27:00	20°32.697'S 176°11.016'W	Cliff, Fissure
	③	2.326 (+0.010)	2,535	08/15 02:58:50	20°32.932'S 176°09.375'W	Cliff
FDC-08	①	2.448 (+0.039)	2,020	08/15 21:37:15	21°24.877'S 176°22.854'W	Fissure
	②	2.420 (+0.017)	2,019	08/15 22:12:35	21°24.778'S 176°22.257'W	
	③	2.419 (+0.019)	2,059	08/15 22:33:20	21°24.823'S 176°21.884'W	Fissure
FDC-09	①	2.667 (+0.050)	1,564	08/17 22:10:30	21°52.986'S 176°45.410'W	
	②	2.514 (+0.023)	1,841	08/18 00:23:45	21°55.042'S 176°44.132'W	
	③	2.677 (+0.077)	1,495	08/18 01:40:20	21°56.203'S 176°43.529'W	Mn-oxides
FDC-10	①	2.452 (+0.022)	1,770	08/18 20:16:30	21°33.641'S 176°16.095'W	Fe-oxides
	②	2.382 (+0.011)	2,107	08/18 20:47:35	21°24.153'S 176°16.207'W	Cliff

FDC－01

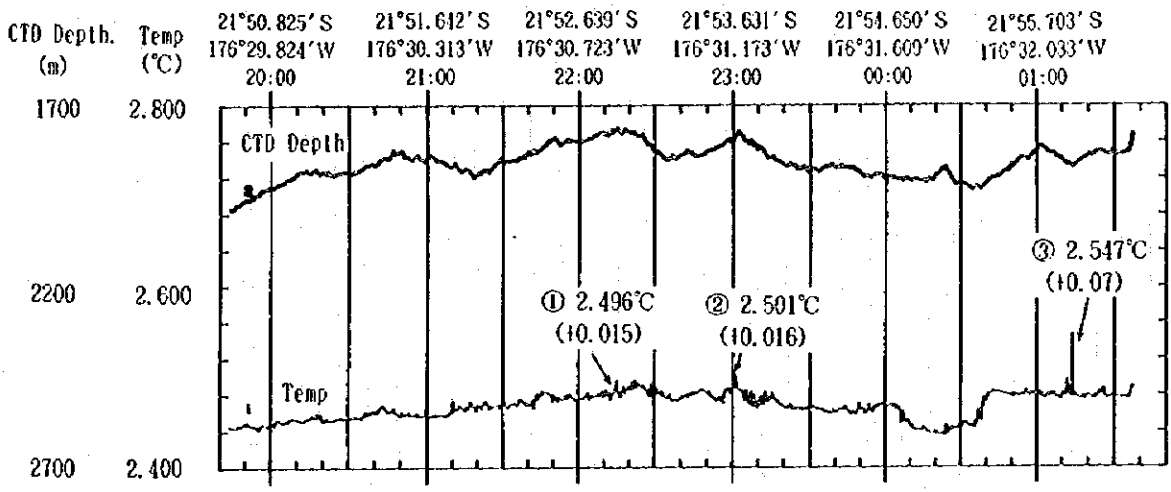

FDC－05

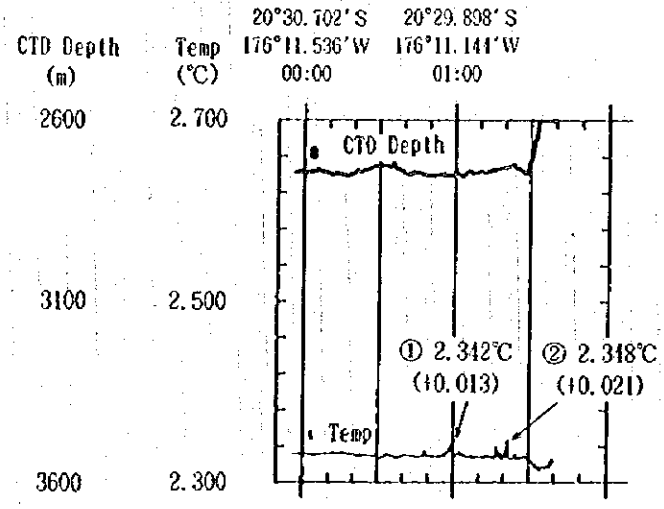

Fig. 4-5-1 (1) Temperature and CTD depth profile

FDC－07

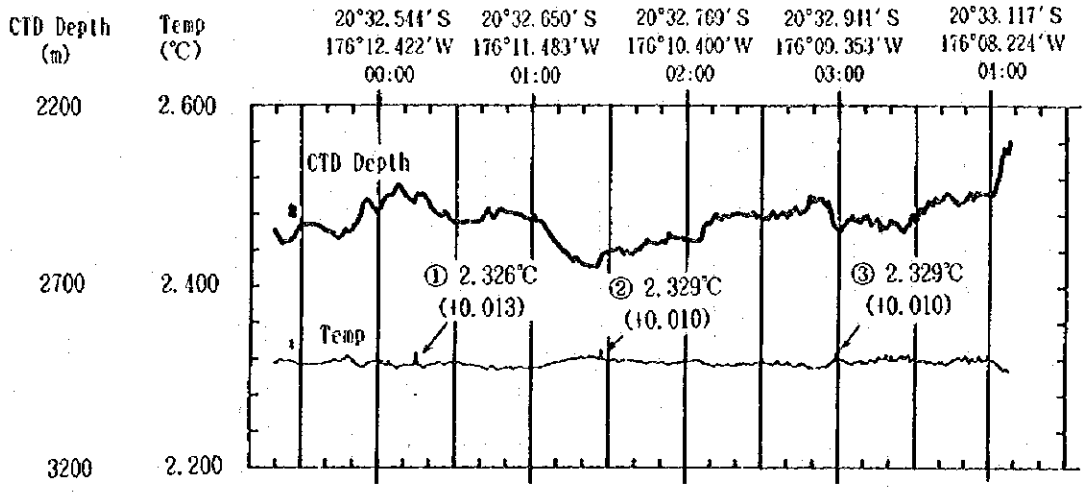

FDC－08

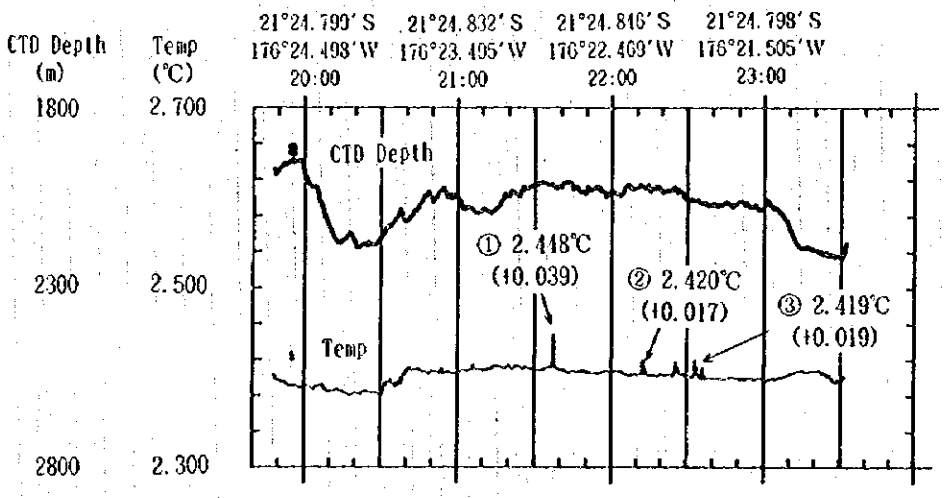

Fig. 4-5-1 (2) Temperature and CTD depth profile

FDC－09

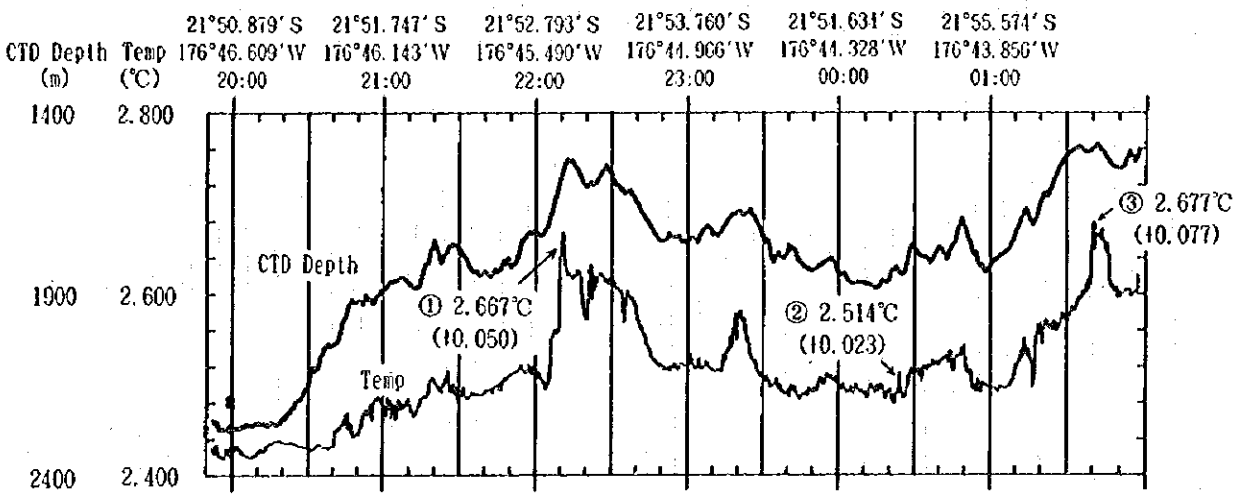

FDC－10

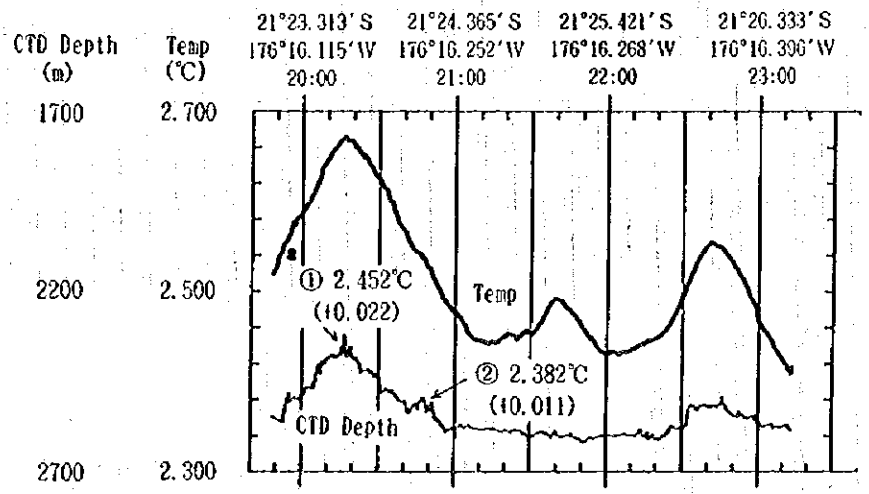

Fig. 4-5-1 (3) Temperature and CTD depth profile

CHAPTER 5 RESULTS OF CHEMICAL ANALYSIS AND OBSERVATIONS

5-1 Microscopic Observation of Thin Section

Description of the typical samples collected by LC, FPG and CB was conducted by a microscope. Thin sections of 17 samples collected at all the 14 sites were prepared. When samples of different lithology were collected at the same site, thin sections of each lithological facies were prepared. The results of microscopic observation and photographs of typical samples are, respectively, shown in Table 5-1-1 and Fig. 5-1-1 (1), (2).

All the samples show a different magnetic intensity. Some of them, such as samples 95SCB07T1 and 95SCB11T are strongly magnetic. The color of these samples varies froin gray, dark gray to greenish dark gray.

The microscopic observation suggests that all these samples are basalt and based on the texture and occurrences of phenocryst, they are classified into three types of basalt. They are aphyric basalt, hypersthene augite basalt and olivine hypersthene augite basalt. Descriptions of each type are given below.

(1) Aphyric basalt

This type is characterized by rare occurrences of phenocrysts and the hand specimen of this type shows no clear phenocrysts. Six samples of 95SLC12T, 95SEPG02T, 95SCB03T, 95SCB06T, 95SCB07T2 and 95SCB09T are included in this type. The groundmass of this type, consisting of abundant glass with common occurrences of euhedral plagioclase, hypersthene and augite, shows variolitic, spherulitic and intersertal textures. The phenocrysts are tiny and euhedral grains of plagioclase and augite, which rarely occur. These are generally vesicular and no alteration minerals are found.

(2) Hypersthene augite basalt

This type is characterized by a lack of olivine phenocrysts and six samples of 95SLC20T, 95SCB05T1, 95SCB05T2, 95SCB07T1, 95SCB08T and 95SCB10T are included in this type. Some of vitreous basalt show spherulitic texture, and the other samples show variolitic or intersertal textures. Plagioclase, hypersthene and augite commonly occur as phenocrysts and the groundmass consists of the same mineral assemblages as phenocrysts. 95SCB05T2, which does not have plagioclase phenocrysts, is slightly different from other samples. With a small amount of plagioclase even in the groundmass, it is similar to boninite, but it is classified to basalt because of no clinoenstatite. Although all samples do not show the alteration, minute grains of brown minerals rarely occur in the spherulitic glass.

Table 5-1-1 Results of microscopic observation of thin section

Sample No.	Rock name	Texture	Phenocryst										Groundmass										Remarks
			Quartz	K-feldspar	Plagioclase	Biotite	Hornblende	Augite	Hypersthene	Olivine	Fe-minerals		Silica minerals	K-feldspar	Plagioclase	Biotite	Hornblende	Augite	Hypersthene	Olivine	Fe-minerals	Glass	Zircon	
95SLC12T	Aphyric basalt	Variolitic			・										△			△	△			◎		
95SLC20T	Vitric hypersthene augite basalt	Spherulitic			○			△	△						△			・	・			◎		
95SFPG01T	Olivine hypersthene augite basalt	Intersertal						○	△	△					△			△	・		・	○		
95SFPG02T	Aphyric basalt	Variolitic			・			・							△			△	・			◎		
95SFPG03T1	Olivine hypersthene augite basalt	Intersertal						○	△	△					△			△	△		・	△		
95SFPG03T2	Olivine hypersthene augite basalt	Intersertal - Vitric						○	△	△					△			△	△		・	◎		
95SCB03T	Aphyric basalt	Intersertal			△			・							○			△	・		・	△		
95SCB04T	Olivine hypersthene augite basalt	Variolitic			◎			△	△	△					○			△	△			◎		
95SCB05T1	Hypersthene augite basalt	Intersertal , Spherulitic			・			△	△		・				△			△	△		・	○		
95SCB05T2	Vitric two pyroxene basalt	Vitric , Spherulitic			・			△	△						・			・	・			◎		
95SCB06T	Aphyric basalt	Variolitic - Intersertal						・							○			△	・		△	◎		
95SCB07T1	Vitric hypersthene augite basalt	Spherulitic			△			△	△						△			△	△		△	◎		
95SCB07T2	Aphyric basalt	Spherulitic , Vitric			・										△			△	△			◎		
95SCB08T	Vitric hypersthene augite basalt	Vitric - Variolitic			○			△	△						△			△	△		△	◎	・	
95SCB09T	Aphyric basalt	Intersertal			・										◎			○	○		△	△		
95SCB10T	Vitric hypersthene augite basalt	Vitric - Spherulitic			○			△	・						△			・	・			◎		
95SCB11T	Olivine hypersthene augite basalt	Intersertal						○	○	△					○			○	△		△	△		

LEGEND ◎ : Abundant ○ : Moderate △ : a few ・ : few

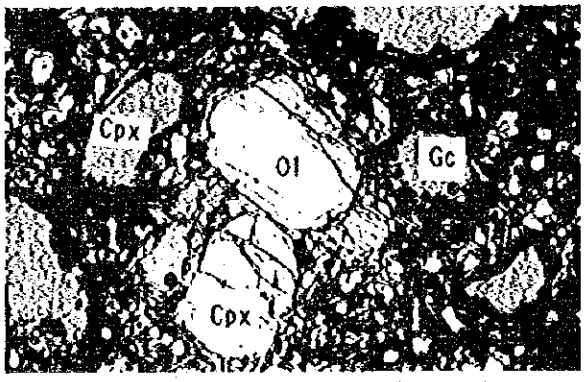

1. 95SFPG01T

Olivine hypersthene augite basalt

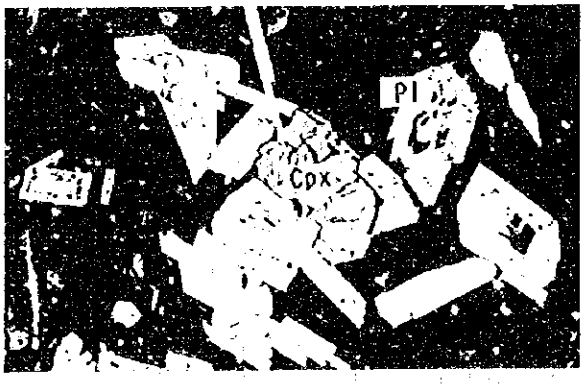

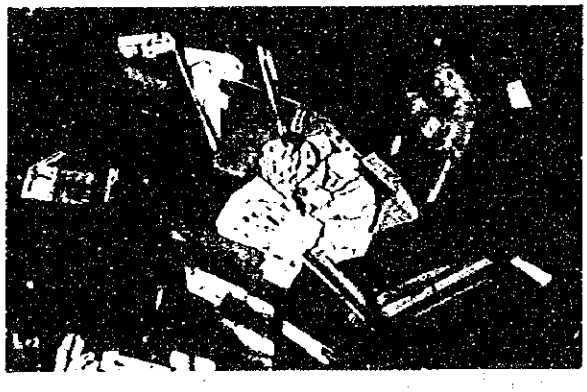

2. 95SCB10T

Glassy hypersthene augite basalt

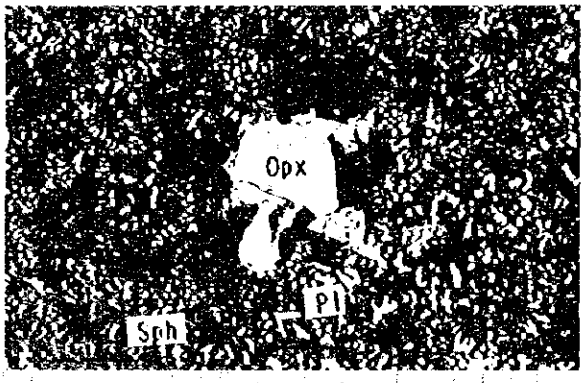

3. 95SCB05T2

Glassy two pyroxene basalt

0 5mm

Left side photos show open nicol,
right side photos clossed nicols.
Legend is shown in next page.

Fig. 5-1-1 (1) Photographs of microscopic observation of thin section

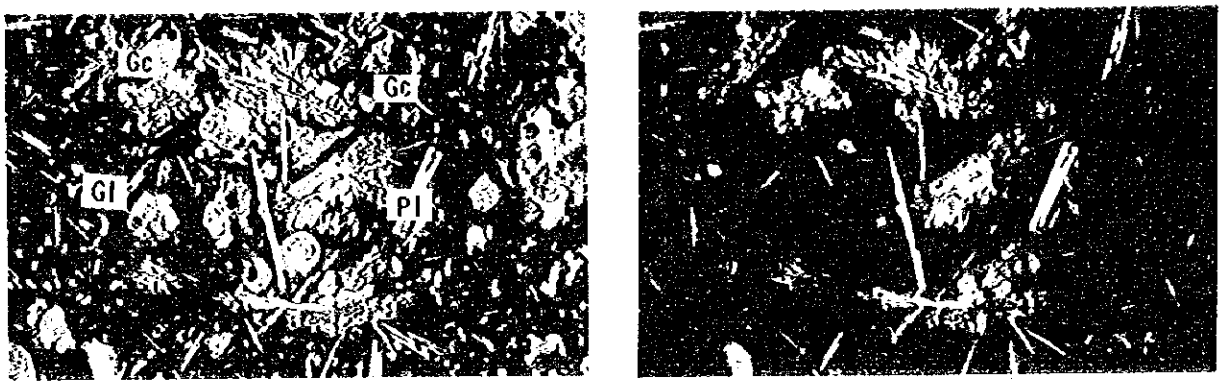

4. 95SFPG02T

Aphyric basalt

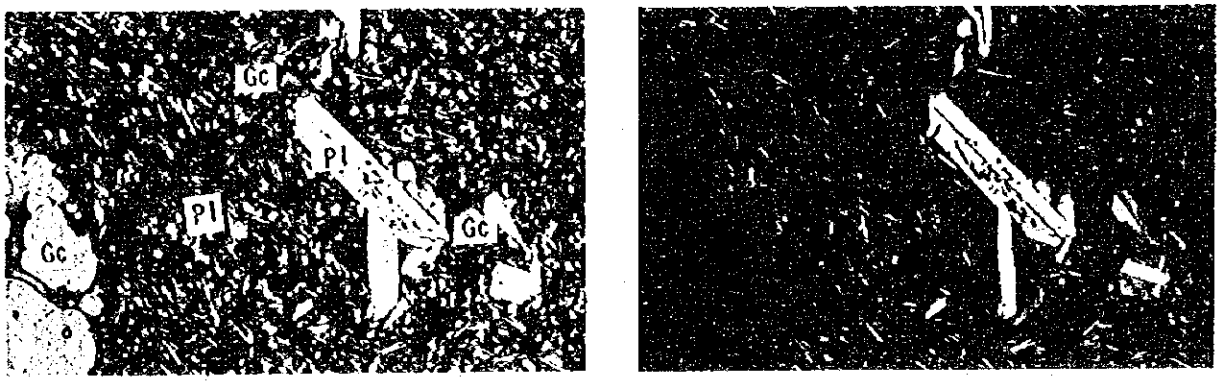

5. 95SCB03T

Aphyric basalt

0 5mm

Left side photos show open nicol, right side photos clossed nicols.

LEGEND

Ol : Olivine
Cpx : Augite
Opx : Hypersthene
Px : Pyroxene
Pl : Plagioclase
Gl : Glass
Sph : Spherulite
Gc : Gass cavity

Fig. 5-1-1 (2) Photographs of microscopic observation of thin section

(3) Olivine hypersthene augite basalt

This type is characterized by olivine phenocryst and five samples of 95SEPG01T, 95SEPG03T1, 95SEPG03T2, 95SCB04T and 95SCB11T are included in this type. Olivine phenocrysts are commonly visible in a hand specimen. The texture of this type is intersertal with the exception of one sample which shows variolitic texture. Plagioclase, hypersthene, augite and a small amount of olivine occur as phenocrysts and the same minerals plus glass and iron oxides constitute the groundmass. No alteration is found, but minute grains of brown minerals occur within glass.

5-2 Microscopic Observation of Polish

A weak dissemination of sulfides was observed in the basalt fragments collected by LC at two sites. A polish was prepared for both of the samples for further examination by microscope. The results of microscopic observation and photographs are, respectively, shown in Table 5-2-1 and Fig. 5-2-1.

Both of the samples, 95SLC12T and 95SLC20T, only show a small amount of pyrite. The pyrite is commonly euhedral grain of less than 0.1mm size, and it occasionally shows rounded or shapeless grains. Only a weak mineralization was observed in both of the samples.

5-3 X-ray Diffraction Analysis

A total of three samples; the above two samples with weak sulfides dissemination collected by LC and one sample with brown oxidation collected by FPG, were examined by X-ray diffraction analysis. In addition to non-orientation power method, orientation method by hydraulic elutriation was conducted for all three samples. The results are shown in Table 5-3-1.

The results of X-ray diffraction of three samples reveal only primary minerals of basalt, and no clay minerals and alteration minerals were identified. This, agree with the microscopic observation, suggests that the collected samples are fresh basalt without the significant alteration.

5-4 Dating the Rock

Dating the rock by K-Ar method was conducted for ten samples of the basalt collected by FPG and CB. The results are given in Table 5-4-1.

After the sample preparation procedures, such as crushing, grain size adjustment, rinsing and drying, all magnetic minerals were removed. The content of K was determined by atomic absorption spectrometer and the isotopic ratio of Ar was determined by noble gas mass spectrometer. The decay

Table 5-2-1 Results of microscopic observation of polish

Sample No.	Rock name	Texture	Mineral name						Remarks
			Pyrite						
95SLC12T	Aphyric basalt	Variolitic	※						Some are framboidal pyrite
95SLC20T	Vitric hypersthene augite basalt	Spherulitic	・						

LEGEND ・:few ※: very few

Table 5-3-1 Results of X-ray diffraction analysis

Sample No.	Rock name	Texture	Mineral name						Remarks
			Plagioclase	Augite	Hypersthene				
95SLC12T	Aphyric basalt	Variolitic	○	△					
95SLC20T	Vitric hypersthene augite basalt	Spherulitic	○	△	△				
95SFPG02T	Aphyric basalt	Variolitic	△	△	△				

LEGEND ○: Moderate △: a few

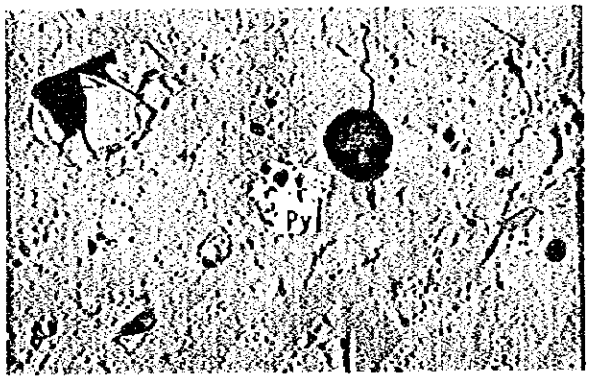

0 1 mm

95SLC20

0 2 mm

95SLC20

0 1 mm

95SLC12

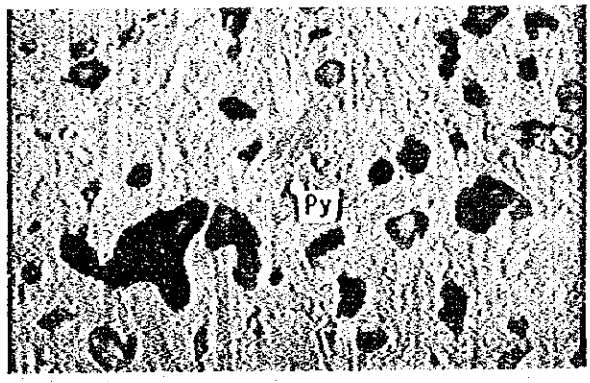

0 1 mm

95SLC12

LEGEND

Py : Pyrite

Fig. 5-2-1 Photographs of microscopic observation of polish

Table 5-4-1 Results of age determination analysis

Sample No.	Sample type	Kalium (wt%)	Rad.40Ar (10^-8 cc/g)	K-Ar age (Ma)	Air contamination (%)	Remarks
95SFPG01K	Whole rock	0.14±0.01	0.30±0.30	0.55±0.55	97.9	
95SFPG02K	Whole rock	0.16±0.01	0.16±0.35	0.25±0.56	99.1	
95SFPG03K	Whole rock	0.10±0.01	0.27±0.33	0.70±0.86	98.3	
95SCB03K	Whole rock	0.25±0.01	0.32±0.53	0.33±0.55	98.8	
95SCB04K	Whole rock	0.03±0.002	3.27±0.52	27.9±4.7	88.1	
95SCB05K	Whole rock	0.08±0.004	0.15±0.56	0.5±1.8	99.5	
95SCB06K	Whole rock	0.18±0.01	0.28±0.98	0.4±1.4	99.4	
95SCB07K	Whole rock	0.03±0.002	4.11±0.66	35.0±5.8	88.1	
95SCB08K	Whole rock	0.04±0.002	1.89±0.52	12.1±3.4	92.8	
95SCB09K	Whole rock	0.24±0.01	1.7±2.1	1.8±2.3	98.4	

Decay constant

$\lambda e = 0.581 \times 10^{-10}$ / Year

$\lambda \beta = 4.962 \times 10^{-10}$ / Year

40K/K = 0.01167 atm%

constant of Steiger and Jaeger (1977) was used for calculation of the ages.

Because of the low content of K and the high ratio of air contamination in all the samples, the accuracy and precision of the obtained ages are low. Three samples with very low K content, 95SCB04K, 95SCB07K and 95SCB08K, give the ages as old as 12 Ma to 35 Ma. Because of the unreasonably old ages for the samples of this geologic situation coupled with very low reliability of these samples, these three samples were disregarded for further consideration. Apart from three samples mentioned above, the interpretation of age determination for seven samples is given below. However, it based on data with low reliability and the error range of them is not given here.

1) Samples on the Spreading Center

The ages of the three samples collected on the spreading center, 95SFPG02K at the south end of the survey area, 95SCB03K at the central south and 95SCB05K at the central north, are, respectively, 0.25 Ma, 0.33 Ma and 0.5 Ma. The ages of the basalt effusion tend to be younger in the south and it increases toward north. These coincide with the evidence that the spreading axis has been extended from north to south and is still extending toward south.

2) Samples in the Surrounding Area of the Spreading Center

Two samples, 95SCB06K and 95SCB09K, were collected in the north part of the survey area where the geological structure parallel to the spreading axis continues. The former sample was collected on the eastern fault scarp in the graben of the spreading center, and the latter was collected on the scarp further away from the spreading center.

The sample 95SCB06K, collected at approximately 2 km east of the spreading center, shows 0.4 Ma. The sample 95SCB09K, collected at approximately 6 km east of the spreading center, shows 1.8 Ma. The increase of the basalt age in accordance with the distance from the spreading center agrees with the spreading movement of the basin.

3) Samples on the Knoll

Two samples, 95SFPG01K and 95SFPG03K, were collected on the knolls in the south end of the survey area where volcanic activities not related to that of the spreading axis took place.

The former sample, collected at approximately 18 km west of the spreading center, shows 0.55 Ma. The latter, collected approximately 17 km east of the spreading axis, shows 0.70 Ma. The older ages of both samples compared with 95SFPG02K (0.25 Ma), which is collected at nearly the same latitude on the spreading center, suggest that these knolls had been formed earlier than the spreading axis.

5-5 Chemical Analysis of Rocks

The chemical analyses were conducted for the rock samples and pyroclastics collected by LC, FPG and CB. Depending on the sample amount and the degree of alteration, the analyzed elements of each sample were chosen from three types of elements combination as shown in Table 5-5-1 and Table 5-5-2. The analytical results and basic statistics are given in Table 5-5-3 (1)-(3).

For the numbering of samples, C1 and C2 were added to LC samples denoting the different depth, while R1 and R2 were added to FPG and CB samples denoting the different lithological facies. The contents inside the parenthesis for LC samples show the sampling depth in centimeters.

(1) Analytical Method

Before the sample preparation, all the samples were rinsed by ultrasonic cleaner and they were dried until they reached a constant weight.

The analytical methods and analyzed elements are given below.

· ICP:	SiO_2, TiO_2, Al_2O_3, Fe_2O_3, MnO, MgO, CaO, Na_2O, K_2O, P_2O_5, Au, Ag, As, Sb, Cs, Ca, Ba, Cu, Pb, Zn, Mn, Fe, Co, Ni, Cr, Cd, Rb, Sr, Ba, Zr, V, Nb, Y, La, Ce, Pr, Nd, Sm, Eu, Gd, Tb, Dy, Ho, Er, Tm, Yb, Lu
· Neutralization Titration:	FeO
· XRF:	S
· LECO:	CO_2

(2) Analytical Results

The analytical results are given below on the basis of each group of analyzed elements.

1) Major Elements (Al, chemical compositions of rocks)

The analytical results of major elements reflect the lithological facies. The basalt with olivine phenocrysts of 95SFPG01R and 95SFPG03R show higher MgO and lower SiO_2, TiO_2, Al_2O_3, FeO and Na_2O compared with other types. The samples 95SCB04R1 and R2, which include olivine phenocrysts with abundant coarse plagioclase grains, show relatively higher Al_2O_3 and CaO, and lower SiO_2, TiO_2, Fe_2O_3, Na_2O and K_2O. No clear chemical difference of major elements is found between aphyric basalt and two pyroxenes basalt.

Table 5-5-1 Analytical components

Group	Kind of component	Component name	Detection limit of analysis
A1	Major component	SiO_2,TiO_2,Al_2O_3,Fe_2O_3,FeO,MnO,MgO,CaO	0.01%
		Na_2O,K_2O,P_2O_5,CO_2	
A2	Minor component	Sr,Ba,Zr,V,Y	1ppm
		Rb,Nb,La,Ce,Pr,Nd	0.1ppm
		Sm,Eu,Gd,Tb,Dy,Ho,Er,Tm,Yb,Lu	0.01ppm
A3	Minor component	Au(2ppb)	described left
		Ag(0.02ppm),Sb(0.2ppm),Cs(0.1ppm),S(50ppm)	described left
		Ca,Ba,Cu,Pb,Zn,Mn,Fe,Co,Ni,Cr,Cd	1ppm

Table 5-5-2 Analytical components and sample No.

Analytical component group	No. of sample	Sample No.
A1+A2+A3	15	95SLC20R,95SFPG01R,95SFPG02R,95SFPG03R, 95SCB03R1,95SCB03R2,95SCB04R1,95SCB04R2, 95SCB05R1,95SCB05R2,95SCB06R,95SCB07R1, 95SCB07R2,95SCB08R,95SCB09R
A1+A2	8	95SLC20CN,95SCB08CN,95SLC08C1(60-65cm), 95SLC10C1(15-20cm),95SLC10C2(40-45cm), 95SLC13C1(60-65cm),95SLC13C2(100-105cm), 95SLC14C1(15-20cm)
A2+A3	1	95SFPG02E
A3	1	95SLC12M

Table 5-5-3 (1) Results of chemical analysis of rocks

(1) Major components : 13 components

Element	SiO_2	TiO_2	Al_2O_3	Fe_2O_3	FeO	MnO	MgO	CaO	Na_2O	K_2O	P_2O_5	CO_2	LOI	Total
Unit	%	%	%	%	%	%	%	%	%	%	%	%	%	%
95SLC20 R	50.74	0.90	15.53	0.01	13.50	0.17	8.04	12.61	2.23	0.07	0.07	0.09	0.01	103.96
95SFPG01 R	47.13	0.56	12.90	1.95	6.50	0.15	12.98	11.85	1.76	0.31	0.10	0.11	3.11	99.41
95SFPG02 R	47.81	0.79	14.86	1.74	7.10	0.16	5.75	9.86	2.41	0.28	0.10	0.07	9.23	100.16
95SFPG03 R	49.70	0.37	11.26	1.90	7.00	0.16	13.26	10.17	1.08	0.24	0.05	0.09	4.47	99.75
95SCB03 R1	51.50	1.35	14.28	2.97	8.80	0.20	4.29	8.46	2.97	0.37	0.15	0.09	4.65	100.08
95SCB03 R2	52.81	1.39	14.76	2.45	9.70	0.20	4.44	8.69	3.09	0.34	0.15	0.09	1.36	99.47
95SCB04 R1	49.87	0.69	17.43	0.99	7.70	0.16	8.23	13.33	1.98	0.04	0.05	0.08	0.01	100.55
95SCB04 R2	49.76	0.69	17.45	0.33	8.30	0.16	8.18	13.34	1.94	0.05	0.05	0.11	0.01	100.36
95SCB05 R1	49.79	0.77	15.41	1.65	7.30	0.16	8.41	12.52	1.98	0.10	0.07	0.10	1.78	100.04
95SCB05 R2	50.97	0.90	15.37	0.89	8.50	0.18	8.01	12.03	2.08	0.15	0.08	0.10	0.29	99.55
95SCB06 R	51.90	1.66	14.51	2.39	10.00	0.21	5.65	9.47	3.11	0.32	0.17	0.10	0.10	99.59
95SCB07 R1	51.50	0.83	15.61	0.87	8.50	0.17	8.31	12.55	2.14	0.10	0.06	0.08	0.01	100.73
95SCB07 R2	50.72	0.84	15.81	0.21	9.00	0.17	8.17	12.54	2.20	0.11	0.07	0.15	0.01	99.99
95SCB08 R	51.66	0.95	15.28	2.52	7.40	0.17	7.63	12.20	2.28	0.15	0.07	0.13	0.01	100.45
95SCB09 R	50.40	1.22	15.30	4.45	7.80	0.19	4.69	9.50	2.93	0.52	0.11	0.26	2.85	100.22
95SLC20 CN	51.33	0.92	15.77	0.01	9.70	0.17	8.04	12.49	2.26	0.04	0.07	0.11	0.01	100.91
95SCB08 CN	51.98	1.20	14.58	0.01	11.40	0.20	6.75	11.05	2.55	0.10	0.10	0.10	0.01	100.02
95SLC08 C1	56.48	0.61	14.56	1.13	8.60	0.18	3.96	8.69	3.06	0.59	0.11	0.28	1.88	100.13
95SLC10 C1	56.72	0.60	14.53	1.24	8.50	0.18	3.81	8.74	2.90	0.60	0.12	0.30	1.80	100.04
95SLC10 C2	55.92	0.65	14.45	1.17	8.90	0.20	3.91	8.99	2.91	0.55	0.11	0.57	1.94	100.27
95SLC13 C1	56.89	0.61	14.55	1.88	7.90	0.18	3.78	8.68	3.01	0.58	0.11	0.34	1.82	100.33
95SLC13 C2	56.78	0.63	14.75	1.49	8.30	0.18	3.96	8.81	2.88	0.56	0.12	0.34	1.62	100.42
95SLC14 C1	56.61	0.59	14.79	1.66	8.00	0.18	3.96	8.73	3.03	0.54	0.11	0.46	1.83	100.49
Maximum	56.89	1.66	17.45	4.45	13.50	0.21	13.26	13.34	3.11	0.60	0.17	0.57	9.23	103.96
Minimum	47.13	0.37	11.26	0.01	6.50	0.15	3.78	8.46	1.08	0.04	0.05	0.07	0.01	99.41
Mean	52.13	0.86	14.95	1.47	8.63	0.18	6.70	10.67	2.47	0.29	0.10	0.18	1.69	100.30
Standard deviation	2.98	0.32	1.25	1.07	1.53	0.02	2.74	1.80	0.54	0.21	0.03	0.14	2.18	0.8888

Table 5-5-3(2) Results of chemical analysis of rocks

(2) Minor elements (REE, etc.) : 21 components

Element	Rb	Sr	Ba	Zr	V	Nb	Y	La	Ce	Pr	Nd	Sm	Eu	Gd	Tb	Dy	Ho	Er	Tm	Yb	Lu
Unit	ppm	ppm	ppm	ppm	ppm	ppm	ppm	ppm	ppm	ppm	ppm	ppm	ppm	ppm	ppm	ppm	ppm	ppm	ppm	ppm	ppm
95SLC20 R	1.4	84	7	51	231	0.73	24	1.71	5.74	0.96	5.42	2.13	0.82	3.12	0.64	3.69	0.80	2.66	0.41	2.61	0.37
95SFPG01 R	6.76	149	32	28	180	0.39	15	2.48	6.66	1.04	5.74	1.97	0.67	2.53	0.42	2.51	0.55	1.63	0.28	1.62	0.23
95SFPG02 R	5.45	134	56	41	230	0.58	21	2.7	7.32	1.18	6.2	2.31	0.78	3.12	0.52	3.39	0.82	2.26	0.35	2.52	0.35
95SFPG03 R	4.04	95	51	19	204	0.14	10	1.06	2.78	0.44	2.36	0.86	0.32	1.20	0.24	1.54	0.35	1.09	0.17	1.25	0.16
95SCB03 R1	5.84	133	68	74	315	1.81	33	3.94	11.3	1.81	9.65	3.34	1.15	4.74	0.94	5.32	1.18	3.60	0.58	3.74	0.53
95SCB03 R2	6.35	136	72	78	323	1.77	35	3.92	11.4	1.8	9.54	3.55	1.29	4.88	0.93	5.61	1.25	3.83	0.61	3.87	0.58
95SCB04 R1	0.91	85	12	41	191	0.66	21	1.51	5.01	0.89	4.99	2.13	0.72	2.88	0.54	3.49	0.79	2.42	0.40	2.68	0.37
95SCB04 R2	1.2	83	10	38	187	0.61	21	1.3	4.55	0.74	4.32	1.58	0.69	2.37	0.50	3.09	0.71	2.30	0.37	2.20	0.34
95SCB05 R1	2.06	91	14	46	219	0.57	24	1.65	5.28	0.88	5.02	1.90	0.76	3.03	0.64	3.57	0.82	2.65	0.39	2.59	0.38
95SCB05 R2	2.89	105	20	50	243	0.63	25	1.91	6.25	1.05	6.02	2.21	0.84	3.36	0.66	4.09	0.85	2.59	0.43	2.89	0.40
95SCB06 R	4.58	112	32	105	303	3.04	43	4.46	13.7	2.15	11.5	4.33	1.40	5.82	1.10	6.73	1.54	4.65	0.75	4.64	0.65
95SCB07 R1	2.14	69	8	46	225	0.92	24	1.58	5.42	0.88	5.18	2.18	0.79	3.27	0.66	4.07	0.90	2.71	0.40	3.00	0.41
95SCB07 R2	2.73	92	10	47	216	0.76	24	1.62	5.42	0.97	5.15	2.05	0.88	3.23	0.63	3.66	0.89	2.62	0.41	2.85	0.38
95SCB08 R	2.31	68	7	47	239	0.7	25	1.54	5.36	0.94	5.4	2.21	0.78	3.14	0.62	3.97	0.87	2.70	0.48	2.86	0.41
95SCB09 R	9.36	199	15	63	330	0.79	33	2.54	8.37	1.44	7.93	3.25	1.16	4.36	0.81	5.13	1.09	3.57	0.57	3.75	0.51
95SLC20 CN	1.17	93	7	53	231	0.68	25	1.74	5.9	1.03	5.88	2.33	0.86	3.18	0.62	4.04	0.87	2.83	0.42	3.12	0.38
95SCB08 CN	1.92	78	13	66	275	1.4	32	2.51	7.98	1.31	7.45	3.21	1.11	4.53	0.85	5.08	1.14	3.69	0.60	3.77	0.55
95SFPG02 E	6.31	142	67	44	228	0.63	24	3.1	8.01	1.25	6.81	2.56	0.91	3.32	0.64	3.78	0.83	2.68	0.43	2.79	0.38
95SLC08 C1	8.21	182	150	30	273	0.34	18	2.38	6.14	0.9	4.82	1.80	0.61	2.13	0.47	2.64	0.67	2.03	0.33	2.14	0.32
95SLC10 C1	8.57	189	158	29	274	0.29	18	2.48	6.39	0.91	5.07	1.89	0.61	2.12	0.44	2.77	0.69	2.22	0.33	2.10	0.35
95SLC10 C2	8.29	190	152	28	296	0.29	18	2.33	5.93	0.92	4.98	1.66	0.57	2.11	0.45	2.85	0.65	2.24	0.34	2.21	0.32
95SLC13 C1	8.07	187	157	31	278	0.25	18	2.5	6.58	0.97	5.23	1.81	0.61	2.24	0.44	2.73	0.72	2.09	0.35	2.21	0.33
95SLC13 C2	8.18	186	156	33	285	0.33	18	2.5	6.44	1	5.24	1.66	0.66	2.30	0.45	2.91	0.69	2.17	0.36	1.99	0.33
95SLC14 C1	8.19	188	154	31	280	0.28	18	2.27	5.92	0.91	4.67	1.80	0.59	2.12	0.46	2.73	0.71	2.02	0.34	2.10	0.32
Maximum	9.36	199	158	105	330	3.04	43	4.46	13.7	2.15	11.5	4.33	1.40	5.82	1.10	6.73	1.54	4.65	0.75	4.64	0.65
Minimum	0.91	68	7	19	180	0.14	10	1.06	2.78	0.44	2.36	0.86	0.32	1.20	0.24	1.54	0.35	1.09	0.17	1.25	0.16
Mean	4.87	128	59	47	252	0.77	24	2.32	6.82	1.10	6.02	2.28	0.82	3.13	0.61	3.72	0.85	2.64	0.42	2.73	0.39
Standard deviatio	2.90	45.6	59.6	19.4	43.9	0.65	7.3	0.86	2.39	0.37	1.96	0.76	0.25	1.08	0.20	1.17	0.25	0.77	0.12	0.79	0.11

Table 5-5-3(3) Results of chemical analysis of rocks

(3) Minor elements (base metal, etc) : 17 components

Element	Au	Ag	As	Sb	Cs	Ca	Ba	S	Cu	Pb	Zn	Mn	Fe	Co	Ni	Cr	Cd
Unit	ppb	ppb	ppm	ppm	ppm	ppm	ppm	ppm	ppm	ppm	ppm	ppm	ppm	ppm	ppm	ppm	ppm
95SLC20 R	1	23.30	0.43	0.1	<0.1	88980	7	1120	98	1	61	1316	104937	44	85	267	1
95SFPG01 R	1	13.40	0.36	0.1	0.1	83618	32	3255	83	1	46	1161	64164	51	264	1270	<1
95SFPG02 R	<1	11.80	0.39	0.1	0.1	69575	56	36530	96	1	66	1239	67359	33	43	48	<1
95SFPG03 R	<1	8.59	0.29	0.1	0.1	71763	51	27420	70	1	55	1239	67701	50	224	801	<1
95SCB03 R1	<1	8.33	0.37	0.1	0.2	59697	68	21235	53	1	92	1549	89177	35	18	20	1
95SCB03 R2	<1	9.09	0.48	0.1	0.2	61320	72	1110	49	1	89	1549	92536	39	13	11	<1
95SCB04 R1	1	19.70	<0.2	0.1	<0.1	94061	12	890	97	1	52	1239	66778	42	117	342	<1
95SCB04 R2	1	21.80	0.25	0.1	0.1	94132	10	785	93	1	48	1239	66825	44	115	365	<1
95SCB05 R1	1	18.50	<0.2	0.1	0.1	88345	14	4650	93	1	55	1239	68285	45	98	349	1
95SCB05 R2	<1	19.00	0.29	0.1	0.1	84888	20	1170	81	1	62	1394	72297	42	87	278	1
95SCB06 R	<1	16.30	0.34	0.1	0.1	66824	32	1750	50	1	93	1626	94448	41	50	132	1
95SCB07 R1	<1	14.30	<0.2	0.2	<0.1	88557	8	3750	101	1	60	1316	72157	44	92	335	1
95SCB07 R2	<1	18.60	0.25	0.1	0.1	88486	10	935	89	<1	59	1316	71427	43	89	322	1
95SCB08 R	<1	27.10	<0.2	0.1	<0.1	86087	7	1025	86	1	64	1316	75147	44	65	212	1
95SCB09 R	<1	9.03	0.4	0.1	0.3	67035	15	1115	44	1	86	1471	91755	41	17	5	1
95SFPG02 E	1	13.90	1.14	0.1	0.2	75291	67	1050	99	1	65	1549	73578	37	41	42	1
95SLC12 M	<1	14.80	0.71	0.1	0.2	74868	61	1920	119	1	70	1471	81491	39	37	86	1
Maximum	1	27.10	1.14	0.2	0.3	94132	72	36530	119	1	93	1626	104937	51	264	1270	1
Minimum	<1	8.33	<0.2	0.1	<0.1	59697	7	785	44	1	46	1161	64164	33	13	5	1
Mean	1	15.74	0.44	0.1	0.1	79031	32	6454	82	1	66	1366	77651	42	86	287	1
Standard deviation	0	5.52	0.24	0.0	0.1	11399	24.8	10874	21.7	0	15.1	142	12312	4.7	68.7	322	0

The comparison of chemical composition between glass part of chilled margin (R2 and CN at the end of sample number) and the central portion (R1 and R at the end of sample number) of the same body shows that the glass is less oxidized with relatively lower Fe_2O_3 and higher FeO. There is no relative difference between them in other chemical compositions except Fe_2O_3 and FeO.

The six sediments samples consisting of black volcanic glass, 95SLC08C1, 95SLC10C1, C2, 95SLC13C1, C2, and 95SLC14C1, show no clear chemical variation between them, however, when compared with basalt, the sediments tend to be higher in SiO_2, K_2O, CO_2 and lower in MgO and CaO.

2) Trace Elements (A2, rare earth elements and related elements)

Three samples of 95SCB03R1,R2 and 95SCB06R, compared with other samples, have higher contents of rare earth elements (from Y to Lu). Since the three samples have no common geological and petrological features and have no difference from others, the reasons for higher concentration of rare earth elements in these samples are unknown. Among other samples than these three, no relative difference in rare earth elements is found. No chemical difference between different rock types and lithological facies is observed in these elements.

The six samples of sediments (C1 and C2 at the end of sample number) show consistently higher Sr and Ba compared with basalt.

3) Minor Elements (A3, base metal and related elements)

Except 95SFPG02E with oxidation and 95SLC12M with sulfide dissemination, all the analyzed basalt samples are fresh. 95SFPG02E and 95SLC12M have relatively higher As and Cu compared with other samples. No relative difference in other elements than As and Cu is found, so that the mineralization concluded from the chemical analysis is not confirmed.

The four samples with olivine phenocrysts, 95SFPG01R, 95SFPG03R, 95SCB04R1 and R2, show relatively higher Ni and Cr and lower Zn, Mn and Fe.

Three samples of 95SFPG01R, 95SFPG03R and 95SCB03R1, show very high S. This reason is unknown, but high S is why three samples show high LOI (major elements analysis).

(3) Classification of Basalt

The chemical compositions of the seventeen basalt samples were considered in various diagrams, such as AFM (Fig. 5-5-1), $MnO-TiO_2-P_2O_5$ (Fig. 5-5-2), Zr-Nb-Y (Fig. 5-5-3), SiO_2-K_2O (Fig. 5-5-4) and chondrite normalized pattern (Fig. 5-5-5). The six sediments samples (C1 and C2 at the end of sample number) were excluded from these considerations.

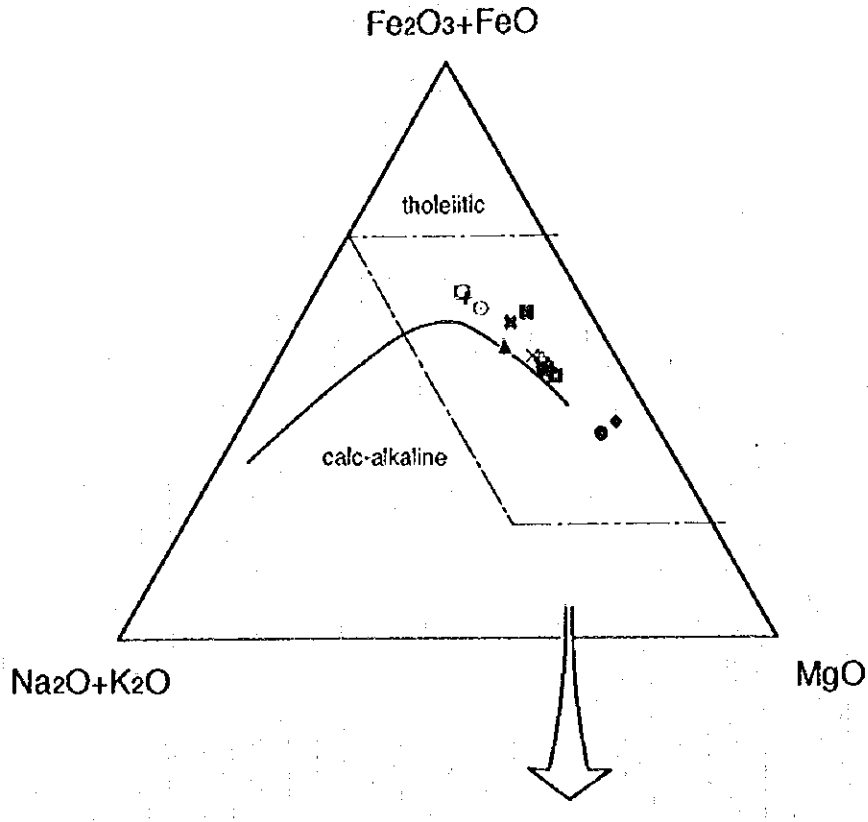

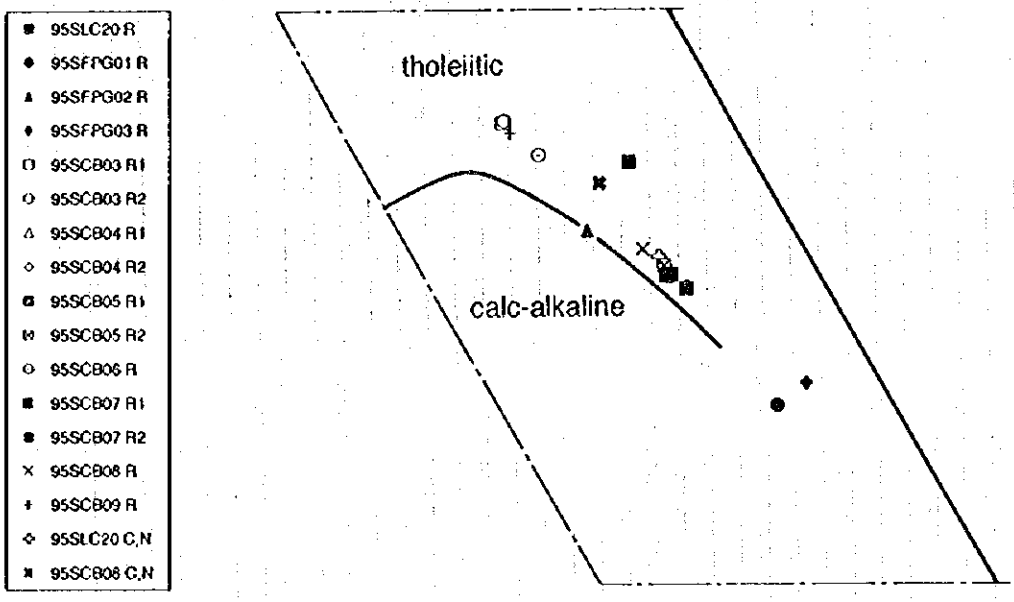

The boundary is from Wilson (1989)

Fig. 5-5-1 AFM diagram

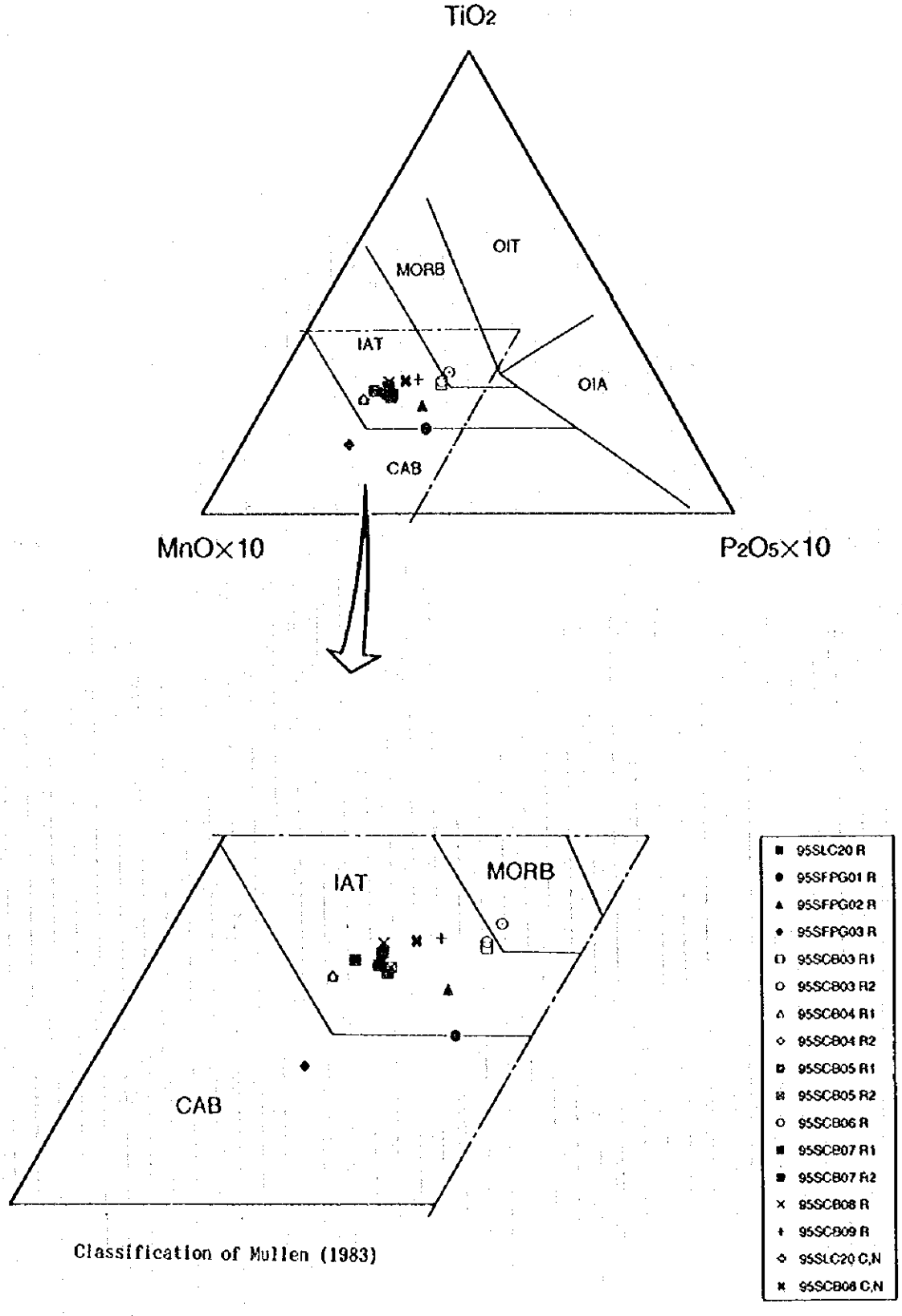

Classification of Mullen (1983)

Fig. 5-5-2 $MnO-TiO_2-P_2O_5$ diagram

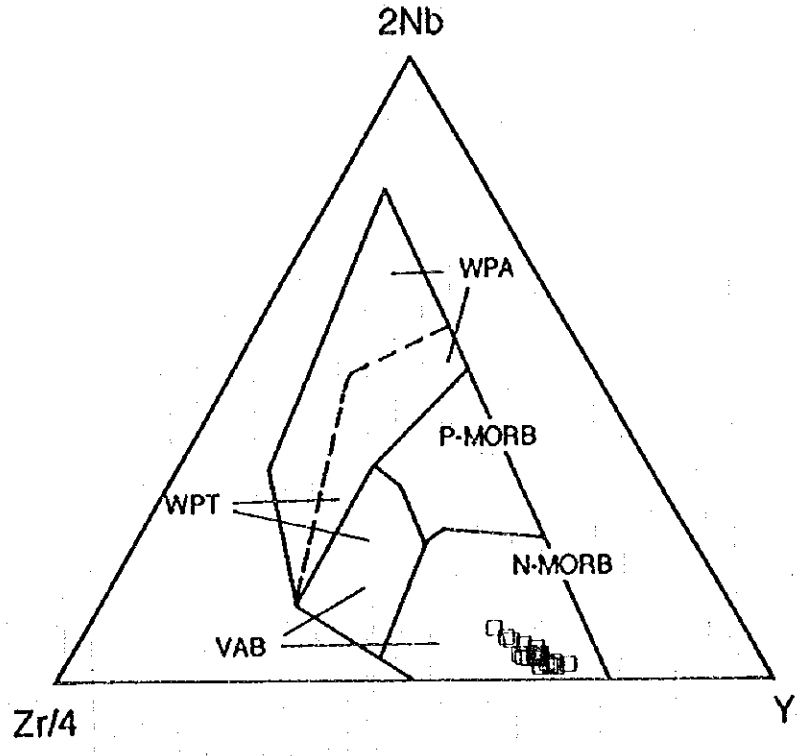

Classification of Meshede (1986)

Fig. 5-5-3 Zr-Nb-Y diagram

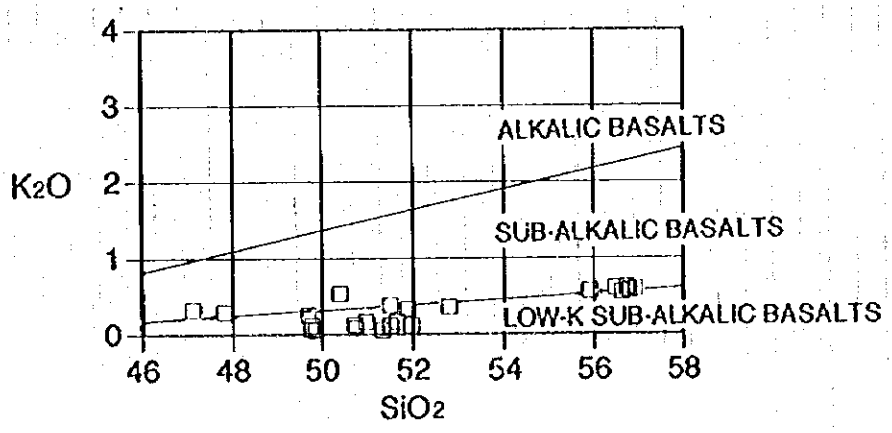

Classification of Midlemost (1975)

Fig. 5-5-4 SiO_2-K_2O variation diagram

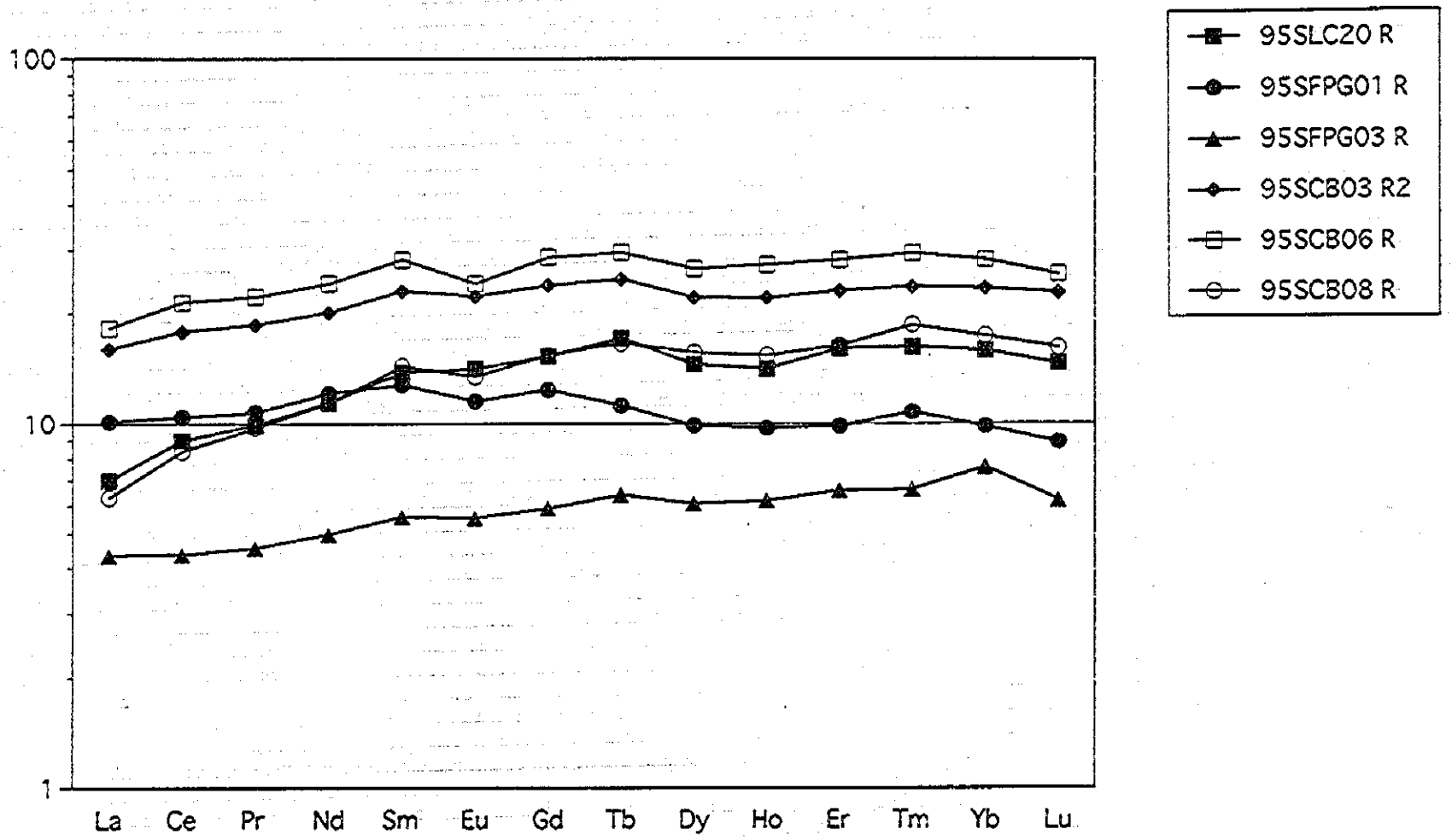

Fig. 5-5-5 REE normalized pattern diagram to chondrite

1) AFM Diagram

Although all the seventeen samples show a scattered distribution, they are plotted in tholeiite field. The two samples, 95SFPG01R and 95SFPG03R, plotted closer to the MgO corner, were collected on the knolls away from the spreading center and they are characterized by olivine phenocrysts. The four samples (95SCB03R1,R2, 95SCB06R, 95SCB09R) are plotted closer to Fe_2O_3+FeO corner. These samples share no common geological and lithological features, but because of higher rare earth elements in them, they also occupy the field separated from others in the chondrite normalized pattern diagram.

2) MnO–TiO_2–P_2O_5 Diagram

95SCB06R is plotted in the field of mid–ocean ridge basalt (MORB), while 95SFPG01R and 95SFPG03R are plotted in the field of calc–alkaline basalt (CAB). All other samples except these three are classified as island–arc tholeiite (IAT).

3) Zr–Nb–Y Diagram

All the samples are plotted in the field corresponding to either volcanic arc basalt (VAB) or normal mid–ocean ridge basalt (N–MORB). The volcanic arc basalt (VAB) is, almost synonymous with island–arc tholeiite (ITA).

4) SiO_2–K_2O Diagram

Because of the lower K_2O content in all the samples, almost all the samples are plotted in the field of LOW K SUB–ALKALIC BASALTS.

5) Chondrite Normalized Pattern Diagram

All the samples show the same chondrite normalized patterns as that of the normal mid–ocean ridge basalt (N–MORB). They are classified into three types of characteristic patterns. Only six typical samples are shown in Fig. 5–5–5. The composition of CI chondrite given by Evensen et al. (1978) is used for the chondrite normalization.

- Group A: Patterns show the moderate slope between La and Sm, and descend to the left (depleted in light–REE).

  11 samples: 95SLC20R,CN, 95SCB04R1,R2, 95SCB05R1,R2 95SCB07R1,R2
  95SCB08R,CN, 95SCB09